Gibbs-Bogolyubov inequality and transport properties for strongly coupled Yukawa fluids

G. Faussurier[1,*] and M. S. Murillo[2]
[1]*Département de Physique Théorique et Appliquée, CEA/DAM Ile-de-France, Boîte Postale 12, F-91680 Bruyères-le-Châtel, France*
[2]*Plasma Theory Group, Theoretical Division, Los Alamos National Laboratory, Los Alamos, New Mexico 87545*
(Received 24 January 2003; published 28 April 2003)

The Gibbs-Bogolyubov inequality is used to establish a mapping between the Yukawa system and both the hard-sphere and the one-component reference systems. The transport coefficients of self-diffusion, shear viscosity, and thermal conductivity are computed for the Yukawa fluid using known properties of the reference systems. Comparisons are made with simulation results. For sufficiently strong screening, the hard-sphere reference system yields a lower upper bound of the Yukawa Helmholtz free energy and a better estimate of the Yukawa transport coefficients.

DOI: 10.1103/PhysRevE.67.046404 PACS number(s): 52.25.Fi, 52.25.Kn, 52.27.Gr

I. INTRODUCTION

When the properties of a many-body system are not known, or are difficult to calculate, it is common to relate the system to another *simpler* reference system and use the known properties of that system. Most often, the relationship between the systems is found using a variational approach such as the Gibbs-Bogolyubov inequality (GBI). The GBI yields a lower upper bound on the Helmholtz free energy of the system of interest in terms of properties of the reference system. An outcome of the variational procedure is a mapping between parameters of the systems. The hard-sphere (HS) system is often used as the reference, although the one-component plasma (OCP) may be encountered for the Coulomb systems. For example, Ashcroft and Stroud have used known properties of the HS system to compute thermodynamic properties of simple liquid metals [1]. This yields, for example, a mapping between the Coulomb coupling parameter Γ of the one-component plasma and the HS packing fraction η. Screened dense plasmas characteristic of Jovian interiors have been similarly modeled by Galam and Hansen by relating them to the HS and OCP systems [2]. In their comparisons of the Helmholtz free energy, they find that the OCP is a superior reference system than the HS under all conditions considered, in the sense that the OCP yields a lower bound on the free energy than the HS.

Properties other than thermodynamic quantities can also be computed using the mapping that results from the GBI. For example, Iyetomi *et al.* [3] compare accurate radial distribution functions for the screened Coulomb systems obtained from Monte Carlo to those obtained from OCP and HS reference systems. They find that the reference systems yield radial distribution functions similar to the Monte Carlo results. In agreement with Galam and Hansen, they also find that the OCP is a superior reference system to the HS system for screened Coulomb systems. Transport properties have also been computed in this way. The diffusion coefficient for the OCP has been estimated by Tanaka and Ichimaru [4] using the known diffusion coefficient of the HS system and the HS-OCP mapping. The relation between the OCP and HS systems is easily generalized to yield a relation between the Yukawa system, for which the interparticle pair interaction is of the form

$$v_Y(r)=\frac{Z^2e^2}{r}\exp(-\alpha r), \tag{1}$$

and the HS system. Here, e, Z, and α are the electron charge, the ion charge, and an effective inverse screening length, respectively. If we express all lengths in unit of the Wigner-Seitz radius a_{WS}, the interparticle pair interaction v_Y multiply by the inverse temperature β can be read under a more usual and compact expression

$$u_Y(r)=\frac{\Gamma}{r}\exp(-\kappa r), \tag{2}$$

where $\Gamma=\beta Z^2e^2/a_{WS}$ and $\kappa=\alpha a_{WS}$ are dimensionless coupling and screening parameters, $\beta=1/k_BT$, $(4\pi/3)a_{WS}^3\rho_i=1$. $\rho_i=N/\Omega$ is the particle density of the system of N ions contained in the volume Ω, T is the temperature of the system supposed to be in thermodynamic equilibrium, and k_B is the Boltzmann constant. The Yukawa-HS mapping can in turn be used to find a relationship between the OCP and Yukawa systems, as shown by Murillo [5], which should be an improvement since the OCP limit ($\kappa\to 0$) is an exact limit and the OCP generally yields a lower free energy estimate for screened Coulomb systems, as mentioned above [2,3]. In this method the HS system acts only as an intermediate system to establish the Yukawa-OCP mapping. Recently, Clérouin and Dufrêche [6] have shown that this relationship yields satisfactory results for the diffusion coefficient and shear viscosity, as compared to simulation results for dense hydrogen.

Generally we do not know *a priori* how good the mapping given by the GBI is, other than knowing that one reference system may be better (yields a lower upper bound on the free energy) than another. Due to the intense recent interest in systems described by the Yukawa model, we are now in a position to be able to perform careful tests of this variational technique. Dusty plasmas (plasmas containing micron-sized impurities or ''grains'') have provided much of the impetus for these studies, for which the intergrain interaction is

*Corresponding author. Email address: gerald.faussurier@cea.fr

known to be of the Yukawa form [7]. This system is similar to a colloidal system, which can also have Yukawa interactions under suitable conditions [8]; however, the colloidal systems are Brownian systems whose dynamics are strongly affected by the solvent. Here our focus is on transport properties in the absence of damping by background species.

The accuracy of the variational procedure can be ascertained by comparing the variational free energy to recently available simulation results. Hamaguchi and co-workers have given accurate results based on molecular dynamics simulations [9] and Caillol and Gilles have presented similar information using Monte Carlo calculations [10]. The results of the variational principle can then be used to obtain transport coefficients. Hamaguchi and co-workers have performed molecular dynamics simulations of transport properties of Yukawa systems, including both the diffusion coefficient [11] and the shear viscosity [12]. More recently, Salin and Caillol [13] have presented a few molecular dynamics computations of the thermal conductivity and the shear and bulk viscosities of the Yukawa one-component plasma.

In Sec. II, the GBI is reviewed in general and for OCP and HS reference systems. In Sec. III, computational details and results are given for the variational procedure. The resulting Yukawa-OCP mapping is used to compute several transport coefficients in Sec. IV and comparisons are made with simulation results. Section V is the conclusion.

II. VARIATIONAL PROCEDURE

The variational approach using the GBI is briefly reviewed in this section in the context of the Yukawa system. Both the OCP and HS systems are considered as possible reference systems.

A. Review of the Gibbs-Bogolyubov inequality

We wish to estimate the free energy of the Yukawa system, as characterized by $\{\Gamma,\kappa\}$, using the known properties of a reference system, as characterized by some set of parameters $\{\alpha_n\}$. To establish the specific parameters of the reference system $\{\alpha_n\}$ that will best describe the Yukawa system, the variational approach based on the GBI is used. We assume that the particles in the reference system have the same mass and temperature than the Yukawa system.

The Helmholtz free energy $\mathcal{F}_Y$ of the Yukawa system is defined in terms of its Hamiltonian $\mathcal{H}_Y$ as

$$\exp(-\beta\mathcal{F}_Y)=\mathrm{Tr}[\exp(-\beta\mathcal{H}_Y)]. \tag{3}$$

Here the trace operation is defined for a classical system as

$$\mathrm{Tr}[\mathcal{A}]\equiv\frac{1}{N!h^{3N}}\int d^{3N}r\int d^{3N}p\,\mathcal{A}, \tag{4}$$

where h is the Planck constant. Consider an arbitrary phase-space density ρ, which describes the reference system with parameters $\{\alpha_n\}$ and is normalized such that $\mathrm{Tr}[\rho]=1$. The unit ratio $\rho/\rho=\rho\exp[-\ln(\rho)]$ can be inserted into the trace to yield

$$\begin{aligned}\exp(-\beta\mathcal{F}_Y)&=\mathrm{Tr}\{\rho\exp[-\beta\mathcal{H}_Y-\ln(\rho)]\},\\&\equiv\langle\exp[-\beta\mathcal{H}_Y-\ln(\rho)]\rangle_\rho.\end{aligned} \tag{5}$$

Here the average is defined as $\langle\mathcal{A}\rangle_\rho\equiv\mathrm{Tr}[\rho\mathcal{A}]$. It is now possible to write, using the inequality $\langle\exp(\mathcal{P})\rangle_\rho\geqslant\exp(\langle\mathcal{P}\rangle_\rho)$ [14],

$$\langle\exp[-\beta\mathcal{H}_Y-\ln(\rho)]\rangle_\rho\geqslant\exp[\langle-\beta\mathcal{H}_Y-\ln(\rho)\rangle_\rho], \tag{6}$$

or, equivalently,

$$\mathcal{F}_Y\leqslant\langle\mathcal{H}_Y\rangle_\rho+\beta^{-1}\langle\ln(\rho)\rangle_\rho. \tag{7}$$

We would now like to choose an approximate form for ρ and variationally minimize the right-hand side of this equation to optimize the accuracy of using ρ for the Yukawa system. Here, we choose

$$\rho\equiv\frac{\exp(-\beta\mathcal{H}_\rho)}{\exp(-\beta\mathcal{F}_\rho)},$$

$$\exp(-\beta\mathcal{F}_\rho)=\mathrm{Tr}[\exp(-\beta\mathcal{H}_\rho)] \tag{8}$$

to be that of some other many-body system, the ''reference system,'' that has well-known properties. For such a reference system we find that

$$\mathcal{F}_Y\leqslant\mathcal{F}_\rho+\langle\mathcal{H}_Y-\mathcal{H}_\rho\rangle_\rho, \tag{9}$$

which is the GBI [14,15]. Note that the average is over properties of the reference system. Once the optimal ρ is found from this inequality, the right-hand side serves as an approximation for the Yukawa Helmholtz free energy. The degree to which the reference system can estimate the properties of the Yukawa system can be ascertained by the closeness of this estimate to the exact free energy $\mathcal{F}_Y$. From Eq. (9), various thermodynamic quantities can be deduced such as pressure, internal energy, and entropy. Details are given in Appendix A. Though many systems can be used as reference systems, the number of choices is drastically reduced if we take into account the constraints that such a reference system should obey in order to test the GBI efficiently. We must have access to the excess free energy, the excess internal energy, and the radial pair-correlation function over the entire fluid domain. Moreover, the main transport coefficients, i.e., the self-diffusion, the shear viscosity, and the thermal conductivity, must be known analytically in the same conditions. To our knowledge, the HS and the OCP systems are the only many-body systems that can pass this test and can be selected as two possible reference systems.

B. Hard-sphere reference

Consider a HS system composed of N spheres of diameter σ in a volume Ω at temperature T. This system is characterized by pair interactions of the form

$$u_{HS}(r)=\begin{cases}\infty, & r<2\eta^{1/3}\\ 0, & r>2\eta^{1/3},\end{cases} \tag{10}$$

where the HS packing fraction is defined as $\eta=\pi\rho_i\sigma^3/6$. The HS system can be characterized by the single parameter η.

C. One-component plasma reference

The unscreened OCP system of N ions in volume Ω at temperature T, neutralized by a rigid homogeneous background, is characterized by pair interactions of the form

$$u_{OCP}(r)=\frac{\Gamma_{OCP}}{r}. \tag{11}$$

This is Eq. (2) with $\Gamma=\Gamma_{OCP}$ and $\kappa=0$. The OCP system can be characterized by the single parameter Γ_{OCP}.

III. RESULTS FOR THE HELMHOLTZ FREE ENERGY

As shown in Appendix A, Eq. (9) can be rewritten as

$$f_Y^{(ex)}\leqslant f_\rho^{(ex)}-u_\rho^{(ex)}+\frac{\rho_i}{2}\int_0^\infty dr\,4\pi r^2\beta v_Y(r)[g_\rho(r)-1]-\frac{\Gamma\kappa}{2}, \tag{12}$$

where $f_Y^{(ex)}$, $f_\rho^{(ex)}$, and $u_\rho^{(ex)}$ are the Yukawa, the reference system excess free, and the reference system internal energies per particle normalized in terms of k_BT, respectively. $g_\rho(r)$ is the radial distribution function of the reference system. $f_Y^{(ex)}$, $f_\rho^{(ex)}$, and $u_\rho^{(ex)}$ are dimensionless quantities [15]. The right-hand side of Eq. (12) can be minimized with respect to $\eta(\Gamma_{OCP})$ if the reference system is the HS (OCP) system for fixed $\{\Gamma,\kappa\}$. By construction, this procedure contains the OCP as the special case. The term -1 inside the integral is due to the rigid and neutralizing background.

As for the HS system, the approximate Carnahan-Starling (CS) HS excess free energy has been used [16]. The hard-sphere radial distribution function is taken in the Percus-Yevick (PY) approximation with or without the procedure proposed originally by Verlet and Weiss (VW) [17] and extended by Henderson and Grundke (HG) [18] in order to correct two major defects of the PY solution: first, the value at contact $g_{HS}(\sigma)$ is too small; second, the later oscillations have the wrong phase and are too weakly damped. Within the VW and the HG approaches, $g_{HS}(\sigma)$ is correct and has a value in agreement with the Carnahan-Starling equation of state. Moreover, the radial distribution function $g_{HS}(r)$ gives the correct isothermal compressibility, which is also consistent with the Carnahan-Starling equation of state. The resulting radial distribution function fits the ''exact'' computer-generated (Monte Carlo or molecular dynamics) functions to within one percent for all η [15]. Note that this procedure can be adapted to any HS equation of state. In each case, the integral in Eq. (12) can be done analytically [5], as shown in Appendix B.

As for the OCP system, the situation is far more difficult because we do not know any simple, accurate, and consistent analytic expressions for the excess internal energy $u_{OCP}^{(ex)}$, the excess free energy $f_{OCP}^{(ex)}$, and the radial distribution function $g_{OCP}(r)$ that span the entire fluid domain, namely, Γ_{OCP} between 0 and 180. Very precise formulas already exist for $u_{OCP}^{(ex)}$ and $f_{OCP}^{(ex)}$ that have been obtained by fitting very accurate Monte Carlo data [19–21]. Some approximate and semi-empirical expressions for $g_{OCP}(r)$ have been proposed in the litterature [22,23]. Some interpolations from very precise Monte Carlo data have been published for $g_{OCP}(r)$, or at least for the structure factor [24,20]. However, none of these expressions can be used to minimize the right-hand side of Eq. (12) with respect to Γ_{OCP} in the entire fluid domain of the Yukawa plane $\{\Gamma,\kappa\}$. The consistency between the radial distribution function and the equation of state is one point. The other point is related to the curvature of the function

$$\Gamma_{OCP}\rightarrow\Delta f_{\Gamma,\kappa}^{GBI}(\Gamma_{OCP})=f_{OCP}^{(ex)}-u_{OCP}^{(ex)}+\frac{\rho_i}{2}\int_0^\infty dr\,4\pi r^2\beta v_Y(r)\times[g_{OCP}(r)-1]-\frac{\Gamma\kappa}{2}. \tag{13}$$

When $\kappa=0$, this function must have only one minimum for $\Gamma_{OCP}=\Gamma$. This means that the best GBI OCP to a given OCP must be the same OCP. If we start from the Yukawa system $\{\Gamma,\kappa\}$, we must recover the OCP system $\{\Gamma,0\}$ as a particular case, when minimizing the right-hand side of Eq. (12) with respect to Γ_{OCP}. None of the aforementioned expressions for $f_{OCP}^{(ex)}$, $u_{OCP}^{(ex)}$, and $g_{OCP}(r)$ satisfy this rule. In general, the situation is worse with increasing Γ. The more we approach the critical value $\Gamma_c=171.8$ corresponding to the OCP melting [5], the flatter is the function near the minimum. As a consequence, any slight inconsistency or inaccuracy can seriously perturb the function $\Gamma_{OCP}\rightarrow\Delta f_{\Gamma,0}^{GBI}(\Gamma_{OCP})$ and lead to unphysical results (one minimum different from Γ, two minima, or even no minimum at all). In summary, the consistency between $f_{OCP}^{(ex)}$, $u_{OCP}^{(ex)}$, and $g_{OCP}(r)$ and the fact that the function $\Gamma_{OCP}\rightarrow\Delta f_{\Gamma,0}^{GBI}(\Gamma_{OCP})$ has a single minimum in $\Gamma_{OCP}=\Gamma$ constitute a stringent test to study the quality of a given OCP system. It should be noted that for HS reference system, the equivalent function

$$\eta\rightarrow\Delta f_{\Gamma,\kappa}^{GBI}(\eta)=f_{HS}^{(ex)}-u_{HS}^{(ex)}+\frac{\rho_i}{2}\int_0^\infty dr\,4\pi r^2\beta v_Y(r)\times[g_{HS}(r)-1]-\frac{\Gamma\kappa}{2} \tag{14}$$

has always one minimum for the OCP case. Moreover, the three approximations CS-PY, CS-VW, and CS-HG give nearly the same value of η when minimizing the right-hand side of Eq. (12). The difference does not exceed a few percents. Furthermore, the curvature in the vincinity of the minimum is strongly marked, so that the difficulties encountered with the OCP reference system are absent there.

To sum up, we need for the OCP reference system $f_{OCP}^{(ex)}$, $u_{OCP}^{(ex)}$, and $g_{OCP}(r)$ that are self-consistent and match exactly the computer-generated quantities for all Γ_{OCP}

$\in[0,180]$. The ideal solution would be to use the computer-generated quantities directly in-line, while minimizing the right-hand side of Eq. (12) with respect to Γ_{OCP}. However, one has to eliminate this solution for computer-time reason. The same reason prevents ourselves to solve in-line integral equations to get the radial distribution function $g_{OCP}(r)$ from the potential $\beta v_{OCP}(r)=\Gamma_{OCP}/r$. The problem of bridge function or closure brings additional complications [15,25–31]. The situation would be hopeless without the Chebyshev approximation [32,33]. This method consists in expanding a given smooth function, defined in the interval $[-1,1]$, on the Chebyshev polynomials up to order N. For a fixed N, this particular polynomial approximation of functions is better than any other one, because the Chebyshev approximation is very nearly the same polynomial as the minimax polynomial, which (among all polynomials of the same degree) has the smallest maximum deviation from the true function. The minimax polynomial is very difficult to find; the Chebyshev approximating polynomial is almost identical and is very easy to compute. This method can be easily generalized to approximate functions defined in finite or infinite intervals [33] and combined with fast Fourier transform (FFT) to speed up the calculations when N is a power of 2. Last but not the least, we can evaluate, quickly and with high precision, the derivative or integral of the function just as if it were a function that has been Chebyshev-fitted *ab initio* and fit that way many variable functions [32].

We have thus solved the hypernetted chain (HNC) equations with the bridge function proposed by Iyetomi *et al.* [30] for OCP system for $r\in[0,50]$ ($r\in[0,10]$) and $\Gamma_{OCP}\in[0.1,180]$ ($\Gamma_{OCP}\in[0,0.1]$), and expanded the radial distribution function (the short-range part of the screening function [25,30]), considered as a function of Γ_{OCP} and r on the Chebyshev polynomials. The interval $[0,180]$ was split in two intervals, $[0,0.1]$ and $[0.1,180]$, to avoid the Gibbs phenomenon due to the stiffness of $g_{OCP}(r)$ near the origin with decreasing Γ_{OCP}: 256 (32) polynomials were used for Γ_{OCP} for the largest (shortest) interval. For the shortest interval, the radial distribution function is taken to be identically null beyond ten. As for r, 256 (32) polynomials were used for the largest (shortest) interval. Clearly, knowing the radial distribution for $32+256$ different values of Γ_{OCP} in the radial range $[0,50]$ allows ourselves to know the radial distribution function as if we had solved the corresponding integral equations in the same interval whatever the value of Γ_{OCP} may be. The storage capacity is limited to the minimum without loss of accuracy due to interpolation procedure or approximate semiempirical analytical fit. All the computing time is spent in generating the data basis, but this work is done once for all! We could have expanded rather the short-range part of the direct correlation function, which is smoother than the radial distribution function for $\Gamma_{OCP}\in[0,180]$. Yet, one should have to perfom an FFT to obtain $g_{OCP}(r)$ by solving the Ornstein-Zernike equation [25,15]. This procedure has the main drawback of slowing down the minimization of the right-hand side of Eq. (12) unnecessarily. Note that this method is neither limited to the OCP system nor to integral equations. One could imagine to use it for other potential and for other method to get the radial distribution function (Monte Carlo, molecular dynamics, HMSA [28], . . .). Finally, $u_{OCP}^{(ex)}$ is calculated by quadrature from $g_{OCP}(r)$ and $f_{OCP}^{(ex)}$ is obtained by running coupling-constant integration from $u_{OCP}^{(ex)}$. Both $u_{OCP}^{(ex)}$ and $f_{OCP}^{(ex)}$ are developed on 256(32) Chebyshev polynomials for $\Gamma_{OCP}\in[0.1,180]$ ($\Gamma_{OCP}\in[0,0.1]$).

TABLE I. Values of Γ_{OCP} minimizing the function $\Delta\mathcal{F}_{\Gamma,0}^{GBI}(\Gamma_{OCP})$ [see Eq. (15)] for different values of Γ. Four cases are considered, depending on how the three terms of the right-hand side of Eq. (15) are calculated, (a) the three terms are calculated by quadrature, (b) the first term is calculated using the fit of DeWitt and Slattery [21] and the two other terms are calculated by quadrature, (c) only the last term is calculated by quadrature, the other terms are taken from the fit [21], (d) the whole terms are calculated from the fit [21]. Γ_c is the critical coupling strength corresponding to the Yukawa liquid-solid phase boundary. $\Gamma_c=171.8$ for OCP [5].

Γ		1.000	10.00	40.00	80.00	160.0	Γ_c
Γ_{OCP}	(a)	1.000	10.00	40.00	80.00	160.0	Γ_c
	(b)	1.009	10.59	41.82	82.10	159.8	170.9
	(c)	0.992	10.71	41.15	83.00	170.8	$>\Gamma_c$
	(d)	1.000	10.00	40.00	80.00	160.0	Γ_c

As an illustration, let us start from Eq. (13) with $\kappa=0$ and let us find the minimum of the function

$$\Gamma_{OCP}\rightarrow\Delta f_{\Gamma,0}^{GBI}(\Gamma_{OCP})=f_{OCP}^{(ex)}-u_{OCP}^{(ex)}+\frac{\Gamma}{\Gamma_{OCP}}u_{OCP}^{(ex)}, \tag{15}$$

in the following four cases, depending on how the three terms of the right-hand side of Eq. (15) are calculated: (a) the three terms are calculated by quadrature, (b) the first term is calculated using the fit of DeWitt and Slattery [21] and the two other terms are calculated by quadrature, (c) only the last term term is calculated by quadrature, the other terms are taken from the fit [21], (d) the whole terms are calcnulated from the fit [21]. Results are written in Table I. Γ_c is the critical coupling strength corresponding to the Yukawa liquid-solid phase boundary. The OCP value $\Gamma_c=171.8$ is taken to be consistent with simulation results [5]. Only cases (a) and (d) give $\Gamma_{OCP}=\Gamma$ up to the OCP liquid-solid phase boundary. In case (b), we are using a reference excess free energy inconsistent with the radial pair-correlation function, but the first-order correction, namely, $\langle\Gamma/r-\Gamma_{OCP}/r\rangle_{\Gamma_{OCP}}=(\Gamma/\Gamma_{OCP}-1)u_{OCP}^{(ex)}$ [see Eqs. (2), (9), and (15)], is calculated self-consistently with the same radial pair-correlation function. Γ_{OCP} is different from Γ but results are good because both values are close to each other and the phase boundary transition is nearly described. In case (c), we are using a reference excess entropy inconsistent with the radial pair-correlation function. Results are similar to case (b) until we approach the phase boundary transition: we thus see that they rapidly deteriorate and the phase boundary transition is not correctly described. In summary, we can use the data obtained by solving the HNC equations with the bridge function proposed by Iyetomi *et al.* [30] (HNC+B) for the OCP

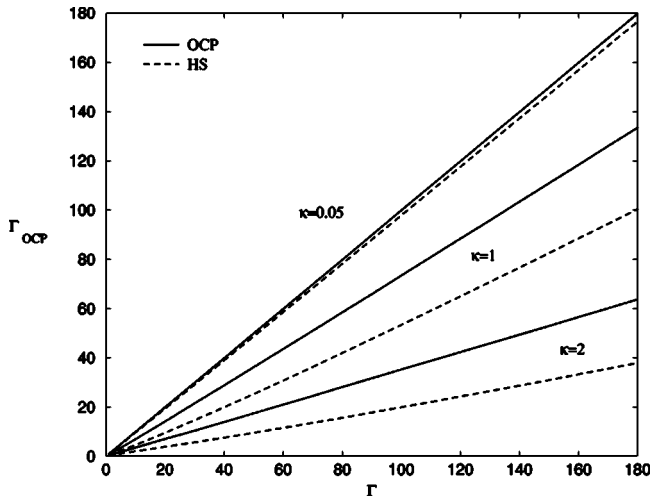

FIG. 1. The OCP coupling parameter versus the Yukawa parameter for various κ values and for HS and OCP reference systems.

system in a self-consistent way within the GBI method. The HNC+B data reproduce well the OCP system [30] but are not perfect [34,35], the uncertainty being greater for the excess entropy than for the excess free energy.

We propose now to minimize the function $\Gamma_{OCP} \rightarrow \Delta f^{GBI}_{\Gamma,\kappa}(\Gamma_{OCP})$ in Eq. (13) with respect to Γ_{OCP}, find the new OCP-Yukawa mapping, and compare to the old method [5]. Results are plotted on Fig. 1. We have used the cases depicted on Fig. 2 of Ref. [5]. We see that for each value of κ, Γ_{OCP} found with the new method is larger than that found with the old method. This means that using a HS reference system tends to overestimate the screening, especially at low Γ and high κ. Calculations were also performed for $\kappa = 0,1,\ldots,9,10$ and $\Gamma > 1$ to get an analytical expression for the OCP-Yukawa mapping parameter (or effective OCP coupling strength) Γ_{OCP} with respect to the Yukawa parameters Γ and κ. The full set of solutions was fit by the form

$$\Gamma_{OCP} = a(\kappa)\Gamma^{b(\kappa)}, \tag{16}$$

where

$$a(\kappa) = 0.081 + 0.920\left[1 - \exp\left(-\frac{7.816}{(1+\kappa)^{2.774}}\right)\right], \tag{17}$$

and

$$b(\kappa) = 0.084 + 0.923\left[1 - \exp\left(-\frac{18.009}{(1+\kappa)^{1.485}}\right)\right]. \tag{18}$$

Numerical values in Eqs. (17) and (18) were obtained from the data written in Table II. To be complete, the full set of solutions for CS-PY was fit by the form

$$\ln(\eta) = 3\ln(\Gamma) - \ln(8) + [a_2(\kappa) + a_3(\kappa)\ln(\Gamma)] \times \ln\{w[a_0(\kappa)\ln(\Gamma) + a_1(\kappa)]\}, \tag{19}$$

where

$$w(x) = \frac{\exp(x)}{1+\exp(x)}, \tag{20}$$

and

$$a_0(\kappa) = -0.115 - \frac{7.487}{1+\kappa} + \left(-0.329 + \frac{6.754}{1+\kappa} - \frac{0.328}{(1+\kappa)^2}\right) \times \left[1 - \exp\left(-\frac{53.273}{(1+\kappa)^2}\right)\right],$$

$$a_1(\kappa) = 0.540 - \frac{24.249}{1+\kappa} + \left(-0.876 + \frac{25.541}{1+\kappa} - \frac{0.744}{(1+\kappa)^2}\right) \times \left[1 - \exp\left(-\frac{51.771}{(1+\kappa)^2}\right)\right],$$

$$a_2(\kappa) = 7.421 - \frac{49.887}{1+\kappa} + \left(-2.040 + \frac{44.408}{1+\kappa} + \frac{1.938}{(1+\kappa)^2}\right) \times \left[1 - \exp\left(-\frac{47.579}{(1+\kappa)^2}\right)\right],$$

$$a_3(\kappa) = -0.027 + \frac{0.467}{1+\kappa} + \left(0.046 - \frac{0.494}{1+\kappa} + \frac{0.014}{(1+\kappa)^2}\right) \times \left[1 - \exp\left(-\frac{31.914}{(1+\kappa)^2}\right)\right]. \tag{21}$$

Right now, this expression extends the fit originally proposed by Murillo [5]. It is consistent with the OCP limit at low Γ, i.e., $\eta \sim (\Gamma/2)^3$ [36]. We found that the relative error with respect to the analytic result of Stroud and Ashcroft [36] for OCP is less than 20% over the range $\eta = 10^{-9}, 0.6$. Equations (19), (20), and (21) generalize the OCP case to the Yukawa case. Numerical values in Eqs. (21) were obtained from the data written in Table III. From now on, the whole applications are done with the original solutions; the use of any fit is explicitly specified.

Although the above results can be justified by the use of the variational principle, the optimal results of the GBI does

TABLE II. Values of $a(\kappa)$ and $b(\kappa)$, defined by Eq. (16), used to obtain Eqs. (17) and (18).

κ	0	1	2	3	4	5	6	7	8	9	10
$a(\kappa)$	1.000	0.709	0.361	0.225	0.163	0.132	0.114	0.103	0.096	0.091	0.089
$b(\kappa)$	1.000	0.999	0.997	0.917	0.824	0.737	0.662	0.600	0.546	0.501	0.462

TABLE III. Values of $[a_i(\kappa)]_{(i=0,3)}$ defined by Eq. (19), used to obtain Eq. (21).

κ	0	1	2	3	4	5	6	7	8	9	10
$a_0(\kappa)$	-1.503	-0.887	-0.731	-0.700	-0.722	-0.753	-0.767	-0.762	-0.748	-0.727	-0.691
$a_1(\kappa)$	0.220	0.144	-0.017	-0.292	-0.631	-0.930	-1.122	-1.209	-1.243	-1.231	-1.144
$a_2(\kappa)$	1.845	3.143	3.707	3.648	3.333	3.087	3.006	3.054	3.155	3.308	3.577
$a_3(\kappa)$	0.006	0.009	0.015	0.023	0.029	0.030	0.028	0.025	0.022	0.019	0.016

not reveal how close the reference excess free energy is to the actual excess free energy, nor what physical quantity other than the excess free energy can be extracted from the optimal results. To quantify the accuracy, the OCP-Yukawa mapping using GBI serves to predict the liquid-solid phase boundary of the Yukawa fluid and to compare to the simulation data of Hamaguchi *et al.* [9]. The phase boundary is found by solving for the critical coupling strength Γ_c and for various κ the equation

$$\Gamma_c = \Gamma_{OCP}(\Gamma, \kappa), \tag{22}$$

where Γ is the unknown and the OCP Γ_c is kept equal to 171.8. We have done similar calculations for the HS reference solving for the critical HS parameter η_c and for various κ the equation

$$\eta_c = \eta(\Gamma, \kappa), \tag{23}$$

where Γ is still the unknown one and the HS η_c is known to be $\eta_c = 2/3\eta_{cp}$. η_{cp} is the closed-packing fraction $\eta_{cp} = \pi/3/\sqrt{2}$ [37]. This procedure differs from that originally proposed in Ref. [5], which had the drawback of not using directly the properties of the reference system, namely, here the HS packing fraction at freezing. Results are shown in Fig. 2. Compared to Fig. 3 of Ref. [5], the actual procedure adopted for HS reference gives a considerable improvement in predicting the phase boundary. Taking into account the VW or the HG corrections have negligible effects on the results. As for OCP reference system, the agreement with the simulation data is excellent considering the simplicity of the theory. The accuracy of the fit is good too. The differences between both reference systems is more pronounced at low Γ, showing that the OCP provides a better reference system for the Yukawa system in this situation. Moreover, such a correspondence is guaranteed to give the exact $\kappa = 0$ limit, whereas a HS reference does not give such a guarantee.

We have plotted in Figs. 3 and 4 the excess entropy and the excess pressure versus Γ using the OCP reference system. The Yukawa values are taken from the procedure and the fits proposed by Caillol and Gilles [10], whereas the OCP exact values are taken from the fit of DeWitt and Slattery [21]. Results are excellent for excess pressure—even better for excess for free energy and excess internal energy (not shown here)—as long as those quantities are calculated by quadrature using the radial pair distribution function at Γ_{OCP} without forgiving the term $-\Gamma\kappa/2$. Results are wrong if we use the excess free energy, excess internal energy, and excess pressure of the OCP reference system. The situation is different for excess entropy because, by construction, the excess entropy of the OCP reference system is the best approximate of the Yukawa system excess entropy, in the GBI framework. Results for excess entropy are good. Note that the excess entropy of the OCP reference system is below the excess entropy of the Yukawa system as expected [38].

To be complete, let us now see whether the variational free energies based on the HS reference system lie systematically above the variational results based on the OCP [2]. For each Γ, we have searched for values of κ using the GBI such that $f^{GBI}_{\Gamma,\kappa}(\Gamma_{OCP})$ in Eq. (13) equals $f^{GBI}_{\Gamma,\kappa}(\eta)$ in Eq. (14). Results are plotted in Fig. 5. We have kept the phase boundary of Fig. 2 predicted by molecular dynamics simulations of Hamaguchi *et al.* [9] and by the OCP and HS reference systems based on GBI calculations. We see that the liquid part of Yukawa system plane can be divided into two parts. For a given value of Γ, the OCP reference system gives a lower excess free energy (OCP liquid) up to a critical value of κ, beyond which the HS reference system gives a lower excess free energy (HS liquid). This result could be expected *a priori* because for weak (strong) coupling, the OCP (HS) potential is physically closer to the Yukawa potential. This result should be compared to GBI calculations using MC or MD data for the OCP reference system, because of the bias due to our HNC+B scheme.

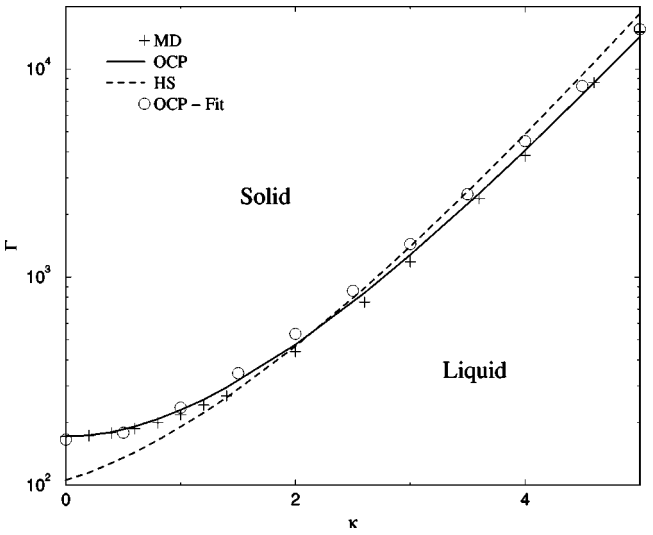

FIG. 2. Phase diagram of the Yukawa system in the $\{\Gamma, \kappa\}$ plane. The liquid-solid phase boundary is shown as predicted by the solution of Eq. (22) for OCP reference system (solid line), the solution of Eq. (23) for HS reference system (dashed line), and the molecular dynamics (MD) results of Hamaguchi *et al.* [9] (cross). The solution of Eq. (22) using the fit of Eqs. (16), (17), and (18) is shown too (circle).

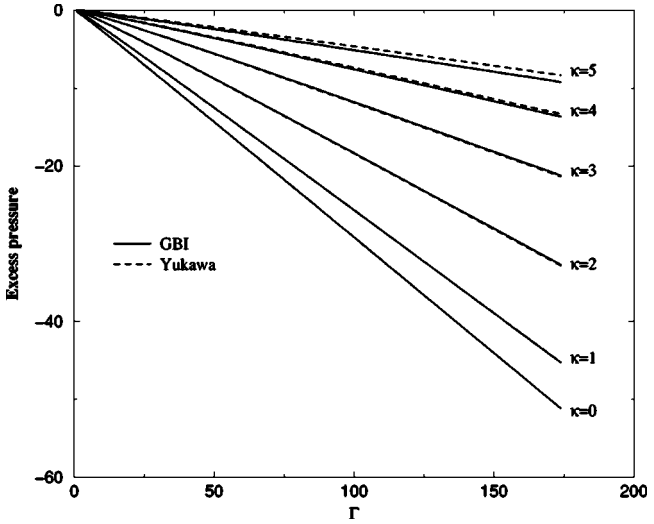

FIG. 3. Excess pressure as predicted by the GBI using the OCP reference system (solid line) and the simulation results for the Yukawa system using the procedure and the fits proposed by Caillol and Gilles [10], whereas the OCP exact values are taken from the fit of DeWitt and Slattery [21].

IV. TRANSPORT COEFFICIENTS

Transport coefficients such as self-diffusion, viscosity, and thermal conductivity are the most fundamental dynamical parameters that reflect the nature of the interparticle potentials and characterize the thermodynamics of the system. The variational approach using the GBI is used in order to estimate the self-diffusion, the shear viscosity, and the thermal conductivity of the Yukawa system from the transport coefficients of the OCP and HS systems. Comparisons with MD data are done in a systematic manner over a wide range of the system parameters $\{\Gamma,\kappa\}$. Our goal is to see whether it is possible to predict dynamic properties of Yukawa systems from the GBI that is only valid to study static properties of systems in thermodynamical equilibrium.

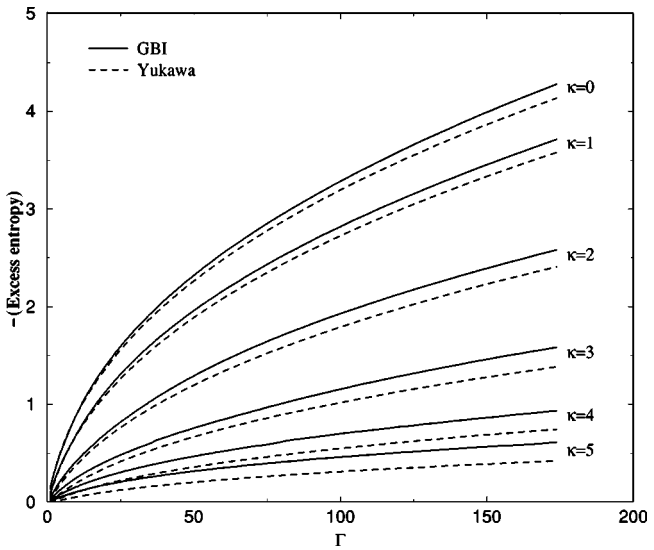

FIG. 4. Minus excess entropy as predicted by the GBI using the OCP reference system (solid line) and the simulation results for the Yukawa system using the procedure and the fits proposed by Caillol and Gilles [10], whereas the OCP exact values are taken from the fit of DeWitt and Slattery [21].

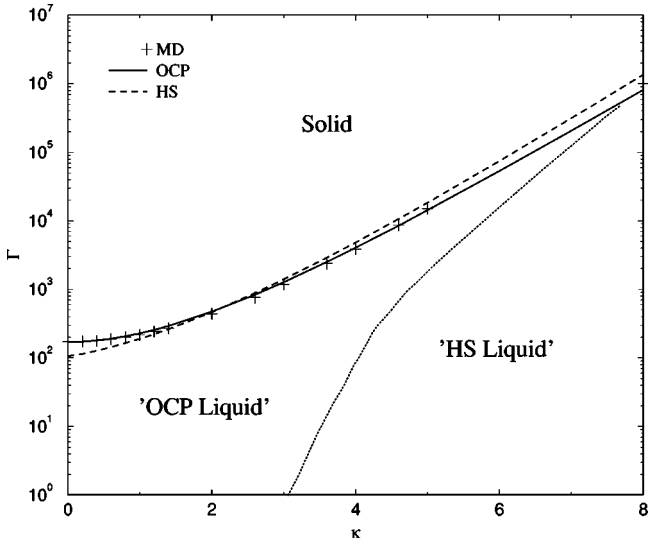

FIG. 5. Phase diagram of the Yukawa system in the $\{\Gamma,\kappa\}$ plane. The "OCP liquid"-"HS liquid" phase boundary (see text, dotted line) is shown with the liquid-solid phase boundary as predicted by the solution of Eq. (22) for OCP reference system (solid line), the solution of Eq. (23) for the HS reference system (dashed line), and the molecular dynamics (MD) results of Hamaguchi *et al.* [9] (cross).

A. Diffusion

The self-diffusion coefficient will be denoted by D. Many conventions exist for normalizing the diffusion coefficient that display quasiuniversal characteristics. Some of these are by Hansen *et al.* [39] $D'=D/D_{pf}$, by Ohta and Hamaguchi [11] $D^*=D/D_{ef}$, and by Rosenfeld [40–43] $D^r=D/D_{md}$, where $D_{pf}=\omega_p a_{WS}^2$, $D_{ef}=\omega_e a_{WS}^2$, and $D_{md}=\rho_i^{-1/3}\sqrt{k_BT/m}$. Here, D_{md}, ω_e, and $\omega_p=\sqrt{4\pi\rho_i Q^2/m}$ are the macroscopic diffusion, the Einstein frequency, and the plasma frequency, respectively. The ratio between the plasma frequency and the Einstein frequency can be obtained from a fit to the result of Ohta and Hamaguchi [11] as

$$\frac{\sqrt{3}\,\omega_e}{\omega_p}=e^{-0.2058\kappa^{1.590}}. \tag{24}$$

Note that the Einstein frequency accounts for variations in the vibration frequency due to screening.

The diffusion coefficient for the OCP is given by [39]

$$D'_{OCP}=\frac{2.95}{\Gamma_{OCP}^{1.34}}. \tag{25}$$

Since $\omega_p/\omega_e=\sqrt{3}$ for OCP system, the OCP reference diffusion normalized in terms of D_{ef} can be defined as

$$D^*_{OCP}\equiv\frac{D_{OCP}}{D_{ef}}=D'_{OCP}\sqrt{3}. \tag{26}$$

The Yukawa diffusion may then be obtained from this OCP result as

$$D^*_{YHMP}(\Gamma,\kappa)=\frac{2.95\sqrt{3}}{\Gamma_{eff}^{1.34}}. \tag{27}$$

In Eq. (27), Y refers to Yukawa and HMP to Hansen, McDonald, and Pollock [39].

However, a log-log plot of D'_{OCP} as a function of Γ_{OCP} is approximately linear and Eq. (25) reproduced the MD data by Hansen *et al.* [39] within 20%, except at the lowest value nearly equal to one. More recently, Ohta and Hamaguchi [11] found that the self-diffusion coefficients in Yukawa systems follow a simple scaling law with respect to the normalized temperature $T^*=\Gamma_c/\Gamma$. In short, T^* is the ratio of the system temperature T to the fluid-solid melting temperature or critical temperature T_c. They fit their MD data to the form

$$D^*=\alpha_\kappa(T^*-1)^{\beta_\kappa}+\gamma_\kappa, \tag{28}$$

for each κ. They were also able to fit the OCP simulation data by Hansen *et al.* [39] to this same and more accurate form, compared to the former power law given by Eq. (25). The Yukawa diffusion may thus be obtained from this new OCP result as

$$D^*_{YOH}(\Gamma,\kappa)=\alpha_0(T^*_{eff}-1)^{\beta_0}+\gamma_0, \tag{29}$$

where $T^*_{eff}=\Gamma_c/\Gamma_{eff}$ with $\Gamma_c=171.8$, i.e., Γ_c used here is the critical Γ of the OCP system as calculated by Hamaguchi *et al.* [9]; Γ_{eff} is given by the GBI variational procedure. In Eq. (29), Y refers to Yukawa and OH to Ohta and Hamaguchi [11].

As for HS system, Enskog's theory for hard sphere is remarkably accurate when compared to simulations [41]. We propose to use a fit to the relatively small corrections to Enskog, as obtained from the most recent simulations for the hard-sphere fluid [44]. Normalizing in terms of D_{ef}, the Yukawa diffusion may be obtained from the HS result D_{HS} as

$$D^*_{YHS}(\Gamma,\kappa)\equiv\frac{D_{HS}}{D_{ef}}=\frac{D_{HS}}{D_E}\frac{D_E}{D_{gas}}\frac{D_{gas}}{D_{ef}}, \tag{30}$$

where

$$\frac{D_{HS}}{D_E}=1.018\,96(1+0.073\eta+11.6095\eta^2-26.951\eta^3),$$

$$\frac{D_E}{D_{gas}}=\frac{(1-\eta)^3}{(1-\eta/2)},$$

$$\frac{D_{gas}}{D_{ef}}=\frac{1}{8\eta^{2/3}}\sqrt{\frac{\pi}{\Gamma}}e^{0.2058\kappa^{1.590}}. \tag{31}$$

Here, D_{gas} and D_E are the result for a dilute gas and Enskog's result, respectively. Note that the CS equation of state for the radial pair distribution function at contact has been used (see Appendix B). This approximation is justified by the fact that the VW and the HG corrections have negligible effects on the Yukawa-HS mapping based on the GBI variational method. In Eq. (30), η is the effective hard-sphere packing fraction of the Yukawa system determined by the GBI variational method. In Eq. (30), Y refers to Yukawa and HS to hard sphere.

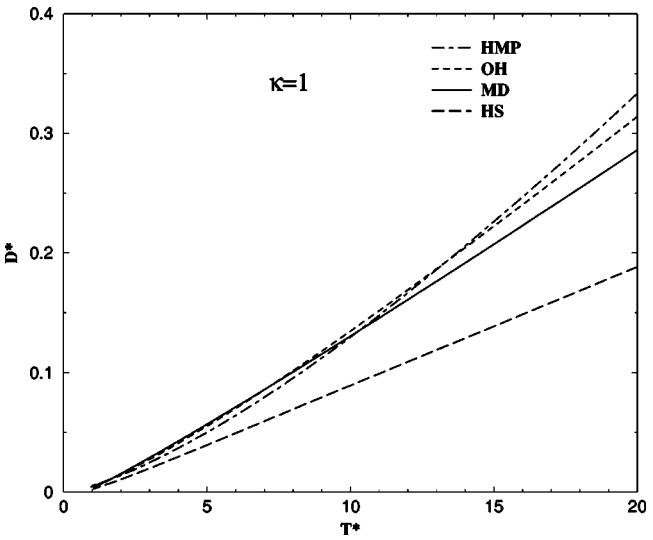

FIG. 6. Self-diffusion coefficient normalized in terms of the Einstein frequency D^* vs normalized temperature T^* of the Yukawa system with $\kappa=1$. MD, OH, HMP, and HS are the MD calculations of Ohta and Hamaguchi [11], the effective OCP using the fit of Ohta and Hamaguchi [11], the effective OCP using the fit of Hansen *et al.* [39], and the effective HS using the analytic formula of Erpenbeck and Wood [41,44].

Results are plotted on Figs. 6, 7, and 8, where the normal-

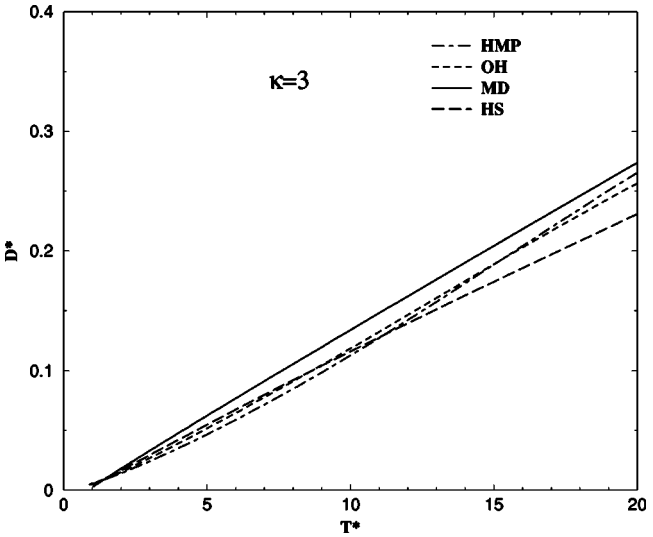

FIG. 7. Self-diffusion coefficient normalized in terms of the Einstein frequency D^* vs normalized temperature T^* of the Yukawa system with $\kappa=3$. MD, OH, HMP, and HS are the MD calculations of Ohta and Hamaguchi [11], the effective OCP using the fit of Ohta and Hamaguchi [11], the effective OCP using the fit of Hansen *et al.* [39], and the effective HS using the analytic formula of Erpenbeck and Wood [41,44].

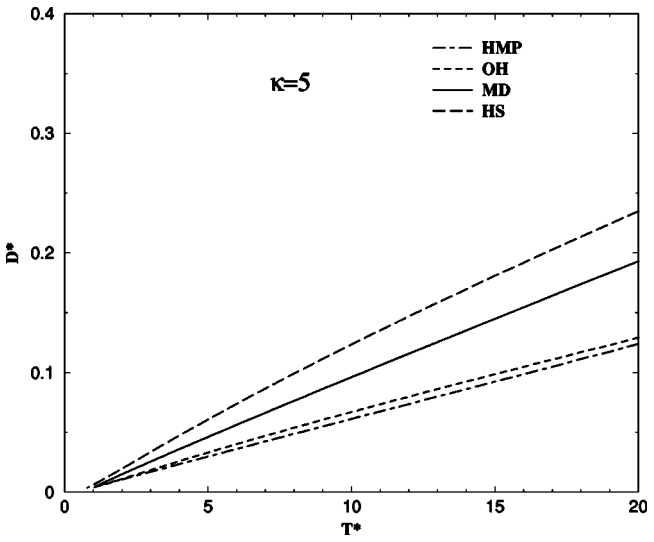

FIG. 8. Self-diffusion normalized in terms of Einstein frequency D^* vs normalized temperature T^* of the Yukawa system with $\kappa=5$. MD, OH, HMP, and HS are the MD calculations of Ohta and Hamaguchi [11], the effective OCP using the fit of Ohta and Hamaguchi [11], the effective OCP using the fit of Hansen *et al.* [39], and the effective HS using the analytic formula of Erpenbeck and Wood [41,44].

ized self-diffusion coefficient D^* is plotted in function of normalized temperature T^* for $\kappa=1,3,5$, respectively. The range of variation of T^* corresponds roughly to the Yukawa system excess entropy above one, i.e., to the strongly coupled Yukawa systems. From Fig. 5, we know that there is a competition between OCP and HS systems, the HS system producing a lower GBI excess free energy with increasing κ at constant Γ. This means that when κ is small (large), the Yukawa system is more OCP-like (HS-like), especially near the liquid-solid phase boundary, i.e., when T^* tends to unity. This is exactly what we find for D^*. For $\kappa=1$, the Yukawa self-diffusion coefficient is better estimated using the OCP system given either by Eq. (27) or Eq. (28) than by the HS system. For $\kappa=3$, the situation changes and HS curve becomes closer to OCP curve; note then that the whole reference systems give roughly the same and good estimate of the Yukawa self-diffusion coefficient. The situation has changed dramatically for $\kappa=5$; as suspected, the HS system gives a better estimate of the Yukawa self-diffusion coefficient over the entire T^* range. The situation is enhanced if we go to higher values of T^* (not shown here). As expected too [43], the whole models converge to the same limit when we approach the liquid-solid phase boundary. To be complete, GBI approach predicts a competition between OCP and HS systems, but the difference between the corresponding GBI excess free energy is indeed tiny. The calculation of self-diffusion confirms this competition, which has a stronger impact on physical results.

B. Viscosity

The shear viscosity will be denoted by η_v to distinguish it from the HS packing fraction η. The definitions of normalized shear viscosities are given by $\eta'=\eta_v/\eta_{pf}$ [15], $\eta^*=\eta_v/\eta_{ef}$ [12], and $\eta^r=\eta_v/\eta_{mv}$ [40–43], where $\eta_{pf}=m\rho_i\omega_p a_{WS}^2$, $\eta_{ef}=m\rho_i\sqrt{3}\omega_e a_{WS}^2$, and $\eta_{mv}=\rho_i^{2/3}\sqrt{mk_BT}$. Here, η_{mv} is the macroscopic viscosity. Note that $\eta^*=\eta'$ when $\kappa=0$, i.e., for the OCP system. The normalization employed for η' has been widely used for the OCP system [15]. The normalization used for η^* has been shown to be more suited for Yukawa systems, and is considered to be a natural extension of η' of the OCP in finite screening (i.e., $\kappa\neq0$) [12].

The viscosity coefficient for the OCP is given by [45]

$$\eta^*_{OCP}=\lambda I_1+\frac{(1+\lambda I_2)^2}{\lambda I_3}, \tag{32}$$

where

$$\lambda=\frac{4\pi}{3}(3\Gamma_{OCP})^{3/2},$$

$$I_1=(180\Gamma_{OCP}\pi^{3/2})^{-1},$$

$$I_2=\frac{0.49-2.23\Gamma_{OCP}^{-1/3}}{60\pi^2},$$

$$I_3=0.241\frac{\Gamma_{OCP}^{1/9}}{\pi^{3/2}}. \tag{33}$$

This analytical fit to the OCP viscosity agrees reasonably with simulation results [46] and represents a procedure for computing the Yukawa viscosity. The Yukawa viscosity may then be obtained from this OCP result as

$$\eta^*_{YWB}(\Gamma,\kappa)=\lambda I_1+\frac{(1+\lambda I_2)^2}{\lambda I_3}, \tag{34}$$

with Γ_{OCP} replaced by Γ_{eff} given by the GBI variational procedure in Eqs. (32) and (33). In Eq. (34), Y refers to Yukawa and WB to Wallenborn and Baus [45].

However, Saigo and Hamaguchi [12] proposed recently a different analytical formula to fit their MD calculations of shear viscosity for Yukawa system that can be used for OCP system as well. η^* can be simply represented for each κ by

$$\eta^*=a_\kappa T^*+\frac{b_\kappa}{T^*}+c_\kappa, \tag{35}$$

where T^* is the normalized temperature defined above. The Yukawa viscosity may thus be obtained from this new OCP result as

$$\eta^*_{YSH}(\Gamma,\kappa)=a_0T^*_{eff}+\frac{b_0}{T^*_{eff}}+c_0, \tag{36}$$

where $T^*_{eff}=\Gamma_c/\Gamma_{eff}$ with $\Gamma_c=171.8$ as for the self-diffusion coefficient. In Eq. (36), Y refers to Yukawa and SH to Saigo and Hamaguchi [12].

As for HS system, Enskog's theory for hard sphere is remarkably accurate when compared to simulations, i.e., for $\eta < \eta_{cp}/5$ [41], except near the liquid-solid phase boundary of the HS system, where the discrepancy may reach a factor of 2 [15,47]. Furthermore, the Stokes relation with slip conditions, i.e., $D\eta_v = k_B T/(2\pi\sigma)$, has been found to be remarquably precise (i.e., for $\eta > \eta_{cp}/5$) [47]. Unfortunately, we do not have more recent MD calculations and neither any analytical expression for the HS shear viscosity. As a consequence, since we know the self-diffusion coefficient for HS system with high precision [41,44], one solution would be to estimate the HS viscosity using the Stokes relation for $\eta > \eta_{cp}/5$ and simply Enskog's result for $\eta < \eta_{cp}/5$, i.e., in the gas phase. However, in order to avoid discontinuity or treat the delicate joining question by a smoooth interpolation between both domains, we propose to use a fit to the corrections to Enskog, as obtained from the simulations for the hard-sphere fluid [47]. The Yukawa diffusion may thus be obtained from the HS result as

$$\eta^*_{YHS}(\Gamma,\kappa) \equiv \frac{\eta_{HS}}{\eta_{ef}} = \frac{\eta_{HS}}{\eta_E}\frac{\eta_E}{\eta_{gas}}\frac{\eta_{gas}}{\eta_{ef}}, \tag{37}$$

where

$$\frac{\eta_{HS}}{\eta_E} = (1 + 2.5502\eta - 23.0982\eta^2 + 44.1238\eta^3),$$

$$\frac{\eta_E}{\eta_{gas}} = \left[\frac{(1-\eta)^3}{(1-\eta/2)} + 0.800(4\eta) + 0.761(4\eta)^2\frac{(1-\eta/2)}{(1-\eta)^3}\right],$$

$$\frac{\eta_{gas}}{\eta_{ef}} = \frac{5}{48\sqrt{3}\,\eta^{2/3}}\sqrt{\frac{\pi}{\Gamma}}e^{0.2058\kappa^{1.590}}. \tag{38}$$

Here, η_{gas} and η_E are the result for a dilute gas and Enskog's result, respectively. Note that the CS equation of state for the radial pair distribution function at contact has been used (see Appendix B). In Eq. (37), η is the effective hard-sphere packing fraction of the Yukawa system determined by the GBI variational method. In Eq. (37), Y refers to Yukawa and HS to hard sphere.

Results are plotted in Figs. 9, 10, and 11, where the shear viscosity η^*, normalized in terms of Einstein frequency, is plotted in function of normalized temperature T^* for $\kappa = 1,3,5$, respectively. The range of variation of T^* is taken from Ref. [12] and covers the strongly and weakly coupled Yukawa systems. First, we see that the analytic fit of Wallenborn and Baus is not good enough to reproduce the MD data. The general feature of the curves is wrong and the viscosity minimum is located too high (low) in $T^*(\Gamma)$ space in any case, even for the OCP system [46]. Second, the competition between the OCP and HS systems is clearly visible. The Yukawa shear viscosity is better estimated using the OCP system [Eq. (35)] than using the HS system [Eq. (37)] for $\kappa = 1$. The opposite is found for $\kappa = 3$. For $\kappa = 5$, we can attribute the shift in amplitude between the HS and MD curves at low T^* either to our approximate formula for HS viscosity or to the known property of viscosity to diverge near the liquid-solid phase boundary [48]. Note that this competition has an impact on the location of the viscosity minimum T^*_m too. When κ increases, the OCP(HS)-like viscosity minimum position T^*_m increases (decreases) and becomes distant (closer) to the MD T^*_m. Finally, we can observe a strong dispersion of the curves above $T^* = 10$.

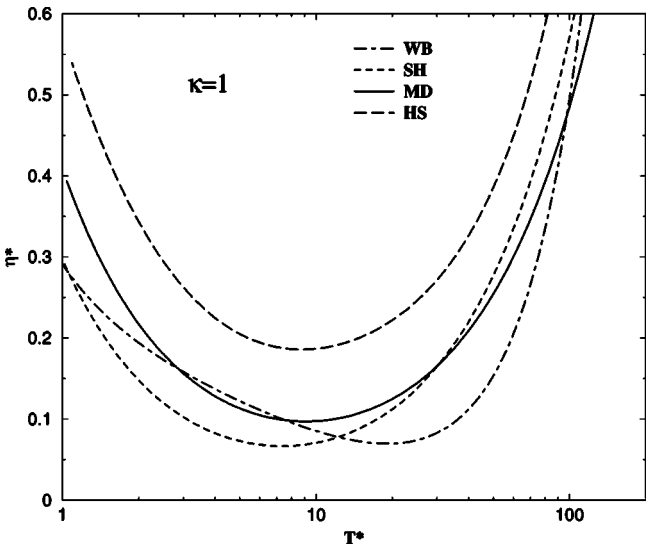

FIG. 9. Shear viscosity normalized in terms of the Einstein frequency η^* vs normalized temperature T^* of the Yukawa system with $\kappa = 1$. MD, SH, WB, and HS are the MD calculations of Saigo and Hamaguchi [12], the effective OCP using the fit of Saigo and Hamaguchi [12], the effective OCP using the fit of Wallenborn and Baus [45], and the effective HS using an analytic formula [15,41,47].

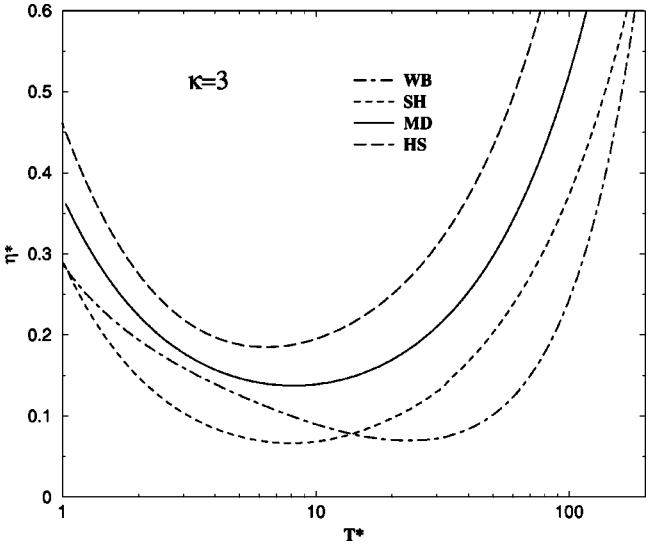

FIG. 10. Shear viscosity normalized in terms of Einstein frequency η^* vs normalized temperature T^* of the Yukawa system with $\kappa = 3$. MD, SH, WB, and HS are the MD calculations of Saigo and Hamaguchi [12], the effective OCP using the fit of Saigo and Hamaguchi [12], the effective OCP using the fit of Wallenborn and Baus [45], and the effective HS using an analytic formula [15,41,47].

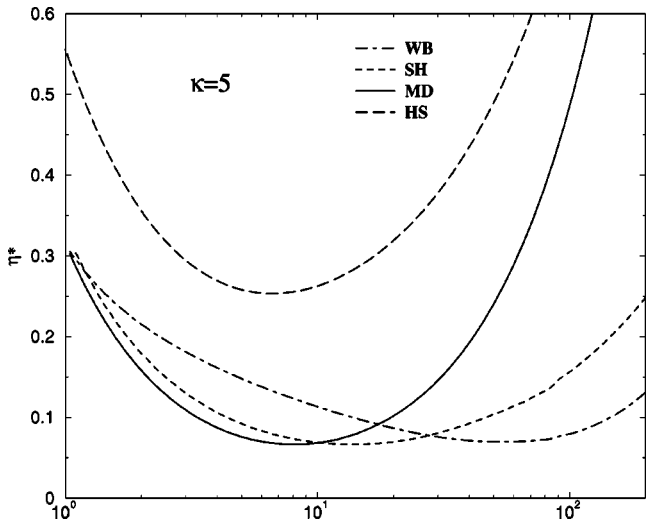

FIG. 11. Shear viscosity normalized in terms of the Einstein frequency η^* vs normalized temperature T^* of the Yukawa system with $\kappa=5$. MD, SH, WB, and HS are the MD calculations of Saigo and Hamaguchi [12], the effective OCP using the fit of Saigo and Hamaguchi [12], the effective OCP using the fit of Wallenborn and Baus [45], and the effective HS using an analytic formula [15,41,47].

We give in Table IV a comparison with the MD data of Salin and Caillol [13] for the shear viscosity η' normalized in terms of the plasma frequency. For the cases considered, the coupling is weak but the competition between the HS and OCP systems is again confirmed. For $\kappa=0,1(\kappa=2,3,4)$ the OCP(HS)-like viscosity gives a better estimate of the Yukawa viscosity than the HS(OCP)-like viscosity. Note that for $\Gamma=2$ and $\kappa=0,1,2$ $(\kappa=3)$, T^* corresponds to the upper limit of (is outside) the interval used by Saigo and Hamaguchi [12] to obtain their fit. Furthermore, for $\Gamma=2,10$ and $\kappa=4$, no fit was proposed and an average formula corresponding roughly to a universal curve is employed. This means that the values given in Table IV for MD^b and OCP should be considered with caution.

C. Thermal conduction

The thermal conductivity will be denoted by λ. The definitions of normalized thermal conductivities are given by $\lambda'=\lambda/\lambda_{pf}$ [15], $\lambda^*=\lambda/\lambda_{ef}$, and $\lambda^r=\lambda/\lambda_{mtc}$ [40–43], where $\lambda_{pf}=k_B\rho_i\omega_p a_{WS}^2$, $\lambda_{ef}=k_B\rho_i\sqrt{3}\omega_e a_{WS}^2$, and $\lambda_{mtc}=\rho_i^{2/3}k_B\sqrt{k_BT/m}$. Here, λ_{mtc} is the macroscopic thermal conductivity [40–43]. Note that $\lambda^*=\lambda'$ when $\kappa=0$. The normalization used for λ^* may be considered to be a natural extension of λ' of the OCP in finite screening.

To our knowledge, no systematic MD calculations over a wide range of the system parameters $\{\Gamma,\kappa\}$ have been carried out [46,13,49] . We have thus decided to fit the most recent and accurate MD data for the OCP system of Donko and Nyiri [46] by the same form selected by Saigo and Hamaguchi for shear viscosity [12]. Thus, the Yukawa thermal conductivity can be simply represented for each κ by

$$\lambda_{YSH}^*(\Gamma,\kappa)=0.011\,76T_{eff}^*+\frac{0.881}{T_{eff}^*}+0.1655, \qquad (39)$$

where $T_{eff}^*=\Gamma_c/\Gamma_{eff}$ with $\Gamma_c=171.8$, as above. From the work of Hamaguchi and co-workers about self-diffusion and shear viscosity, we can assume a quasiuniversal behavior and calculate the Yukawa thermal conductivity from

$$\lambda^*(\Gamma,\kappa)=0.011\,76T^*+\frac{0.881}{T^*}+0.1655, \qquad (40)$$

where T^* is the normalized temperature already encountered. In Eq. (39), *Y* refers to Yukawa and SH to Saigo and Hamaguchi [12].

The situation is less dramatic for the HS system, because the deviations of MD calculations from Enskog's expression have been proven to be barely perceptible within the few percent accuracy of the data [47]. As a consequence, once obtained the effective hard-sphere packing fraction η of the Yukawa system using the GBI variational method, the Yukawa thermal conductivity normalized in terms of λ_{ef} may be estimated from the HS result λ_{HS} as

$$\lambda_{YHS}^*(\Gamma,\kappa)\equiv\frac{\lambda_{HS}}{\lambda_{ef}}=\frac{\lambda_{HS}}{\lambda_E}\frac{\lambda_E}{\lambda_{gas}}\frac{\lambda_{gas}}{\lambda_{ef}}, \qquad (41)$$

where

$$\frac{\lambda_{HS}}{\lambda_E}=1,$$

TABLE IV. Shear viscosity normalized in terms of plasma frequency η' for a few thermodynamics states. MD^a, MD^b, OCP, and HS are given by the MD calculations of Salin and Caillol [46,13], the MD calculations of Saigo and Hamaguchi [12], the effective OCP using the fit of Saigo and Hamaguchi [12], and the effective HS using an analytic formula [15,41,47], respectively. T^* is the normalized temperature.

	$\Gamma=2$					$\Gamma=10$				
κ	T^*	MD^a	MD^b	OCP	HS	T^*	MD^a	MD^b	OCP	HS
0	85.9	~0.5	0.42	0.42	0.47	17.18	~0.1	0.09	0.09	0.22
1	108.7	0.496	0.43	0.51	0.66	21.74	0.112	0.11	0.10	0.19
2	220.05	0.991	0.61	0.63	1.01	44.01	0.145	0.13	0.12	0.21
3	592.	1.282	0.85	0.61	1.45	118.5	0.198	0.19	0.13	0.27
4	1918.	1.935	1.48	0.46	1.98	383.7	0.306	0.29	0.11	0.35

TABLE V. Thermal conductivity normalized in terms of plasma frequency λ' for a few thermodynamics states. MD[a], MD[b], OCP, and HS are given by the MD calculations of Salin and Caillol [46,13], the Yukawa estimation using a fit form of Saigo and Hamaguchi [12], the effective OCP using a fit form of Saigo and Hamaguchi [12], and the effective HS using an analytic formula [15,41,47], respectively. T^* is the normalized temperature.

	$\Gamma=2$					$\Gamma=10$				
κ	T^*	MD[a]	MD[b]	OCP	HS	T^*	MD[a]	MD[b]	OCP	HS
0	85.9	$\sim$1.2	1.19	1.19	1.86	17.18	$\sim$0.40	0.42	0.42	1.07
1	108.7	2.42	1.18	1.37	2.48	21.74	0.570	0.38	0.40	0.84
2	220.05	2.89	1.49	1.59	3.73	44.01	0.644	0.38	0.40	0.82
3	592.0	5.36	2.20	1.50	5.40	118.5	0.841	0.48	0.38	1.00
4	1918.0	7.18	3.53	1.13	7.37	383.7	1.239	0.72	0.29	1.31

$$\frac{\lambda_E}{\lambda_{gas}}=\left[\frac{(1-\eta)^3}{(1-\eta/2)}+1.200(4\eta)+0.755(4\eta)^2\frac{(1-\eta/2)}{(1-\eta)^3}\right],$$

$$\frac{\lambda_{gas}}{\lambda_{ef}}=\frac{25}{64\sqrt{3}\,\eta^{2/3}}\sqrt{\frac{\pi}{\Gamma}}e^{0.2058\kappa^{1.590}}. \tag{42}$$

Here, λ_{gas} and λ_E are the results for a dilute gas and Enskog's result, respectively. Note that the CS equation of state for the radial pair distribution function at contact has been used. In Eq. (41), Y refers to Yukawa and HS to hard sphere.

We give in Table V a comparison with the MD data of Salin and Caillol [13] for the thermal conductivity normalized in terms of the plasma frequency λ'. As above, the coupling is weak but the competition between the HS and OCP systems is clearly visible, even if the values given by MD[b] are too low by a factor of nearly 2 for κ above one. For $\kappa=0$ ($\kappa=1,2,3,4$) the OCP(HS)-like viscosity gives a better estimate of the Yukawa viscosity than the HS(OCP)-like viscosity. Furthermore, these comparisons seem to justify our method and the use of Eqs. (39) and (41), waiting for MD simulations in a wider range of the parameter space to propose a better fit and to confirm the competition between HS and OCP systems for thermal conductivity.

D. Rosenfeld approach

A semiempirical ''universal'' corresponding-states relationship, for the dimensionless transport coefficients of dense fluids as functions of the reduced configurational entropy, has been proposed by Rosenfeld [40], extended to dilute fluids by the same author [41], and established by many simulations [40,50]. This approach is invaluable for four reasons. First, an accurate, theoretically based, approach to dense-fluid transport coefficients is still lacking. Second, no convergent perturbation theory of transport coefficients has been established. Third, the brute-force computer methods can be used to estimate transport coefficients, but these methods are considerably too time consuming, for the same accuracy, than those designed to measure equilibrium properties and cannot be considered as black-box routines that generate data intensively over an industrialized scale. Fourth, this analytical relation between transport coefficients and excess entropy allows us to estimate, for instance, self-diffusion, shear viscosity, and thermal conductivity from the equation of state of monoatomic fluids with arbitrary pair potentials. In summary, one realizes all the benefits of the Rosenfeld approach to estimate transport coefficients knowing only the excess entropy of the system of interest. This method is as useful as Enskog's original recipe relating transport coefficients to thermal pressure [51].

Let us consider a one-component fluid with a reduced excess entropy $s=-S/(Nk_B)$, where S is the entropy of the system of interest composed of N particles in the volume Ω at temperature T. In short, s is equal to minus the reduced excess or configurational entropy over the ideal-gas value. The quasiuniversal behavior for the transport coefficients has been derived either from many simulations for dense fluids [40], or from Enskog's theory for dilute fluids [41] by considering, i.e., normalized self-diffusion D^r, normalized shear viscosity η^r, and normalized thermal conductivity λ^r. Keeping the aforementioned normalization in terms of the Einstein frequency to be consistent with the MD of Hamaguchi *et al.*, the Rosenfeld scaling entropy transport coefficients of self-diffusion D^*_{esc}, shear viscosity η^*_{esc}, and thermal conductivity λ^*_{esc} for Yukawa fluid are given by

$$D^*_{esc}=D^r\frac{D_{md}}{D_{ef}},$$

$$D^*_{esc}=\eta^r\frac{\eta_{mv}}{\eta_{ef}},$$

$$\lambda^*_{esc}=\lambda^r\frac{\lambda_{mtc}}{\lambda_{ef}}, \tag{43}$$

where

$$\frac{D_{md}}{D_{ef}}=\sqrt{3}\,\frac{\eta_{mv}}{\eta_{ef}}=\sqrt{3}\,\frac{\lambda_{mtc}}{\lambda_{ef}}=\frac{e^{0.2058\kappa^{1.590}}}{\sqrt{\Gamma}}\left(\frac{4\pi}{3}\right)^{1/3}. \tag{44}$$

For dense fluids [41],

$$D^r\approx 0.6e^{-0.8s},$$

$$\eta^r\approx 0.2e^{0.8s},$$

$$\lambda^r\approx 1.5e^{0.5s}, \tag{45}$$

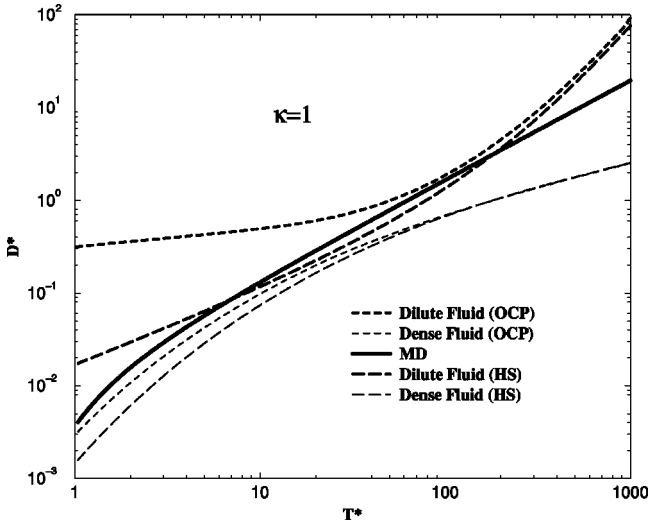

FIG. 12. Self-diffusion coefficient normalized in terms of the Einstein frequency D^* vs normalized temperature T^* of the Yukawa system with $\kappa=1$. The quasiuniversal entropy scaling formulas for dilute and dense fluids proposed by Rosenfeld [40,41] are compared to MD calculations of Ohta and Hamaguchi [11]. HS and OCP reference systems are considered.

whereas for dilute fluids [41], we obtain for HS

$$D^r \simeq 0.37 s^{-2/3},$$

$$\eta^r \simeq 0.27 s^{-2/3},$$

$$\lambda^r \simeq \frac{15}{4}\eta^r, \tag{46}$$

and for OCP

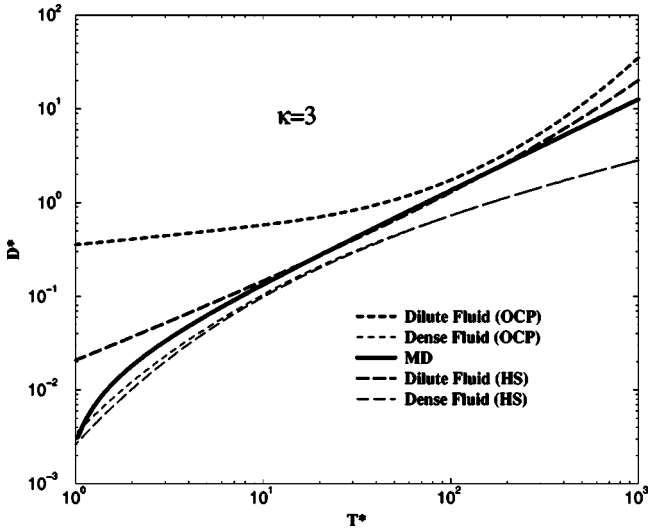

FIG. 13. Self-diffusion coefficient normalized in terms of the Einstein frequency D^* vs normalized temperature T^* of the Yukawa system with $\kappa=3$. The quasiuniversal entropy scaling formulas for dilute and dense fluids proposed by Rosenfeld [40,41] are compared to MD calculations of Ohta and Hamaguchi [11]. HS and OCP reference systems are considered.

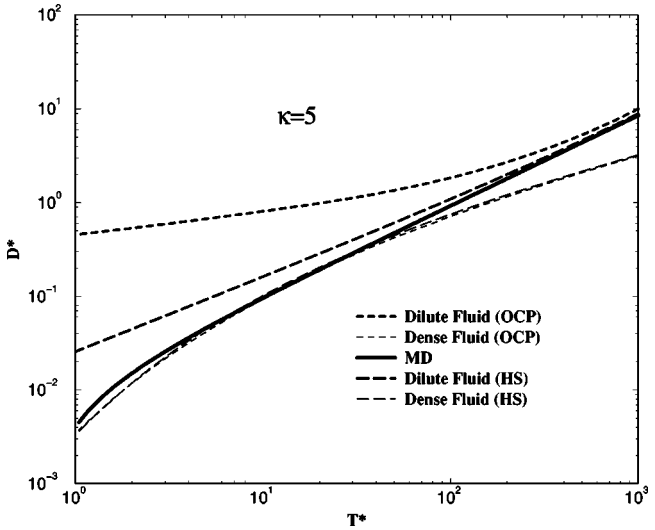

FIG. 14. Self-diffusion coefficient normalized in terms of the Einstein frequency D^* vs normalized temperature T^* of the Yukawa system with $\kappa=5$. The quasiuniversal entropy scaling formulas for dilute and dense fluids proposed by Rosenfeld [40,41] are compared to MD calculations of Ohta and Hamaguchi [11]. HS and OCP reference systems are considered.

$$D^r \simeq \frac{0.40 s^{-4/3}}{\ln\left[1+\left(\frac{2}{3s}\right)^2\right]},$$

$$\eta^r \simeq \frac{0.35 s^{-4/3}}{\ln\left[1+\left(\frac{2}{3s}\right)^2\right]-\frac{1}{1+\left(\frac{3s}{2}\right)^2}},$$

$$\lambda^r \simeq \frac{15}{4}\eta^r. \tag{47}$$

The quasiuniversal behavior for dense fluids, which holds also for the OCP case, is replaced by two different behaviors that depend on the inverse power law of the pair potential for dilute fluids [41].

The elegant and deep method proposed by Rosenfeld relates the transport coefficients to the equation of state via the Gibbs-Bogolyubov inequality. We have thus used the GBI reduced excess entropy for HS and OCP systems to see how the predictions of Eqs. (45), (46), and (47) for self-diffusion and shear viscosity compare to MD simulations. Results are plotted on Figs. 12(15), 13(16), and 14(17), where the self-diffusion coefficient D^* (the shear viscosity η^*), normalized in terms of the Einstein frequency, is plotted in a function of normalized temperature T^* for $\kappa=1,3,5$, respectively. The quasiuniversal entropy scaling formulas for dilute and dense fluids proposed by Rosenfeld [40,41] are compared to MD calculations of Ohta (Saigo) and Hamaguchi for self-diffusion coefficient (shear viscosity) [11] ([12]). HS and OCP reference systems are explicitely considered. First of all, the difference between HS and OCP systems

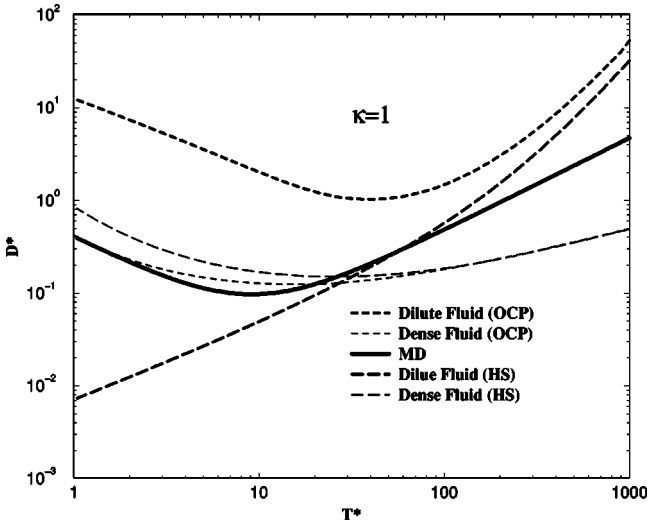

FIG. 15. Shear viscosity normalized in terms of the Einstein frequency η^* vs normalized temperature T^* of the Yukawa system with $\kappa=1$. The quasiuniversal entropy scaling formulas for dilute and dense fluids proposed by Rosenfeld [40,41] are compared to MD calculations of Saigo and Hamaguchi [12]. HS and OCP reference systems are considered.

decreases with increasing κ for dense fluids; for $\kappa \geqslant 3$, one can use one or the other, whatever T^* may be. The same tendency is found for dilute fluids except that T^* must be greater than 100, which corresponds roughly to GBI reduced excess entropy below one, i.e., to the uncoupled Yukawa systems as expected. Second, the competition between HS and OCP systems is again confirmed, $\kappa=3$ being the borderline. Third, the most important result is that MD calculations nicely interpolate between dilute fluid at high T^* and dense fluid at low T^*, the transition between both regimes being

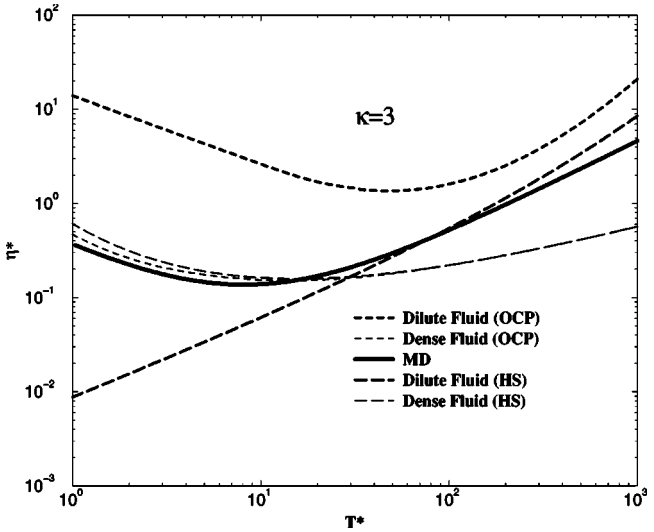

FIG. 16. Shear viscosity normalized in terms of the Einstein frequency η^* vs normalized temperature T^* of the Yukawa system with $\kappa=3$. The quasiuniversal entropy scaling formulas for dilute and dense fluids proposed by Rosenfeld [40,41] are compared to MD calculations of Saigo and Hamaguchi [12]. HS and OCP reference systems are considered.

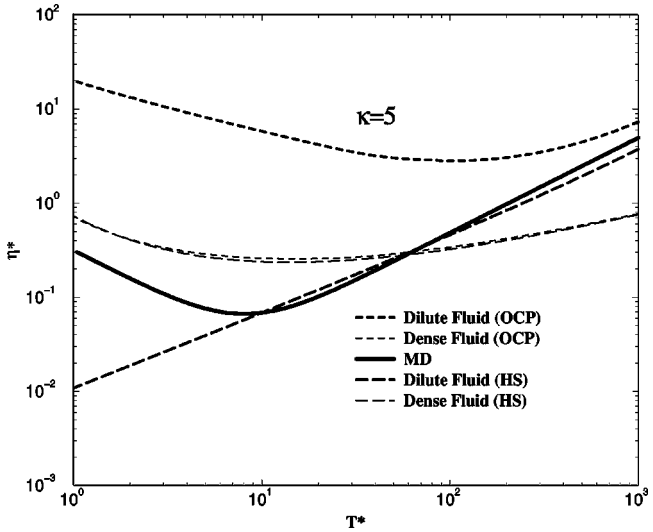

FIG. 17. Shear viscosity normalized in terms of the Einstein frequency η^* vs normalized temperature T^* of the Yukawa system with $\kappa=5$. The quasiuniversal entropy scaling formulas for dilute and dense fluids proposed by Rosenfeld [40,41] are compared to MD calculations of Saigo and Hamaguchi [12]. HS and OCP reference systems are considered.

located between $T^*=10$ and $T^*=100$. One could even predict a minimum for shear viscosity, as already enhanced by Rosenfeld [43].

V. CONCLUSIONS

The Gibbs-Boglyubov inequality is used to map the Yukawa system to either the hard-sphere or the one-component reference systems. This method is very powerful to calculate equation of state quantities, i.e., pressure, internal energy, free energy, and entropy. It has been shown that this method can also be very efficient to estimate transport coefficients, i.e., self-diffusion, shear viscosity, and thermal conductivity. One can employ either the known transport coefficients of the reference systems or the quasiuniversal entropy scaling of Rosenfeld based on a correspondence between transport coefficients and reduced excess entropy. Extensive comparisons are made with simulation results over a wide range of the Yukawa system parameters $\{\Gamma,\kappa\}$. It has been proven that the hard-sphere reference system yields a lower upper bound of the Yukawa Helmholtz free energy and a better estimate of the Yukawa transport coefficients for sufficiently strong screening.

The method presented here is easily extended to other systems and to other properties for which expressions are known for the hard-sphere and one-component systems. Because of the simplicity of the theory, the same method can be applied to mixtures.

ACKNOWLEDGMENTS

One of the authors (G.F.) thanks P. Dallot for providing his HNC code, adapted from a program originally developed by R. Cauble to calculate static correlations for a two-

component plasma (ions and electrons) in the HNC approximation [52].

APPENDIX A: YUKAWA FLUID EQUATION OF STATE FROM THE GIBBS-BOGOLYUBOV INEQUALITY

In this appendix, we derive first Eq. (12) from Eq. (9). Second, we calculate various thermodynamic quantities from Eq. (12) and apply the results to the one-component Yukawa system case.

Starting from Eq. (9) and using $\mathcal{U}_\rho=\langle\mathcal{H}_\rho\rangle_\rho$, we get

$$\mathcal{F}_Y\leqslant\mathcal{F}_\rho-\mathcal{U}_\rho+\langle\mathcal{H}_Y\rangle_\rho \tag{A1}$$

or

$$\mathcal{F}_Y^{(ex)}\leqslant\mathcal{F}_\rho^{(ex)}-\mathcal{U}_\rho^{(ex)}+\langle\mathcal{H}_Y\rangle_\rho, \tag{A2}$$

by subtracting to both sides the ideal free energy $\mathcal{F}^0$ [15]

$$\mathcal{F}^0=+Nk_BT[\ln(\rho_i)+3\ln(\Lambda)-1], \tag{A3}$$

and the ideal internal energy $\mathcal{U}^0$ [15]

$$\mathcal{U}^0=\frac{3}{2}Nk_BT. \tag{A4}$$

Here, Λ is the de Broglie thermal wavelength, defined as

$$\Lambda=\left(\frac{2\pi\hbar^2}{mk_BT}\right)^{1/2}. \tag{A5}$$

The excess parts contain all the contributions to the free and internal energies that arise from the interactions between particles. A similar division into ideal and excess parts can be made for any thermodynamic function obtained by differentiation of the free energy with respect to the temperature T and the volume Ω of the system assumed to be in thermodynamic equilibrium. In order to work with dimensionless quantities per particle, we rather consider reduced free energy $f_\rho^\theta\equiv\beta\mathcal{F}_\rho^\theta/N$ and internal energy $u_\rho^\theta\equiv\beta\mathcal{U}_\rho^\theta/N$ [$\rho=Y,\mathrm{OCP},\mathrm{HS},\ldots$ and $\theta=0,(ex),\ldots$]. We thus get

$$f_Y^{(ex)}\leqslant f_\rho^{(ex)}-u_\rho^{(ex)}+\left\langle\frac{\beta\mathcal{H}_Y}{N}\right\rangle_\rho. \tag{A6}$$

Note that $f_\rho^{(ex)}$ and $u_\rho^{(ex)}$ are often called abusively excess free and internal energies per particle.

The main point is to calculate the thermal average of the configurational energy of our model, $\langle\beta\mathcal{H}_Y/N\rangle_\rho$, which is constituted of a neutral classical plasma made of N identical point charges Z (ions) immersed in a uniform neutralizing background (electrons) of volume Ω and charge density $-\rho_e=-Z\rho_i$. The effective interaction between ions due to the polarization background of electrons $\mathcal{H}_Y$ may be expressed as follows [10],

$$\mathcal{H}_Y=\frac{1}{2}\sum_{i\neq j}Z^2v_\alpha(|\mathbf{r}_i-\mathbf{r}_j|)-\sum_i\int d^3\mathbf{r}\rho_eZv_\alpha(|\mathbf{r}-\mathbf{r}_i|)+\frac{1}{2}\int d^3\mathbf{r}\int d^3\mathbf{r}'\rho_e^2v_\alpha(|\mathbf{r}-\mathbf{r}'|)+N\mathcal{E}, \tag{A7}$$

where $v_\alpha(|\mathbf{r}|)=e^2e^{-\alpha r}/r$ and $i,j=1,\ldots N$. In the right-hand side of Eq. (A7), the first term is the particle-particle interaction, the second one is the particle-background interaction, the third one is the background-background interaction, whereas the last term fixes the zero of energy with respect to the self-energy of a bare Coulomb charge

$$\mathcal{E}\equiv\frac{1}{2}\lim_{r\to0}[Z^2v_\alpha(|\mathbf{r}|)-Z^2v_0(|\mathbf{r}|)]. \tag{A8}$$

Let us now multiply Eq. (A7) by β/N. Using Eq. (2) and the system being isotropic and homogeneous,

$$\frac{\beta\mathcal{H}_Y}{N}=\frac{1}{2N}\sum_{i\neq j}\beta Z^2v_\alpha(|\mathbf{r}_i-\mathbf{r}_j|)-\rho_i\int d^3\mathbf{r}Z^2\beta v_\alpha(|\mathbf{r}|)+\frac{1}{2}\rho_i\int d^3\mathbf{r}Z^2\beta v_\alpha(|\mathbf{r}|)+\beta\mathcal{E}, \tag{A9}$$

we easily obtain

$$\frac{\beta\mathcal{H}_Y}{N}=\frac{1}{2N}\sum_{i\neq j}\beta v_Y(|\mathbf{r}_i-\mathbf{r}_j|)-\left(\frac{3\Gamma}{2\kappa^2}+\frac{\kappa\Gamma}{2}\right). \tag{A10}$$

The excess internal energy per particle $\langle\beta\mathcal{H}_Y/N\rangle_\rho$ is simply given by

$$\left\langle\frac{\beta\mathcal{H}_Y}{N}\right\rangle_\rho=\frac{1}{2N}\left\langle\sum_{i\neq j}\beta v_Y(|\mathbf{r}_i-\mathbf{r}_j|)\right\rangle_\rho-\left(\frac{3\Gamma}{2\kappa^2}+\frac{\kappa\Gamma}{2}\right), \tag{A11}$$

since $\langle1\rangle_\rho=1$. Finally, let us introduce the two-particle density [15] $\delta^{(2)}(\mathbf{r},\mathbf{r}')$

$$\delta^{(2)}(\mathbf{r},\mathbf{r}')=\sum_{i\neq j}\delta(|\mathbf{r}-\mathbf{r}_i|)\,\delta(|\mathbf{r}'-\mathbf{r}_j|), \tag{A12}$$

$$\left\langle\frac{\beta\mathcal{H}_Y}{N}\right\rangle_\rho=\frac{1}{2N}\int d^3\mathbf{r}\int d^3\mathbf{r}'\beta v_Y(|\mathbf{r}-\mathbf{r}'|)\langle\delta^{(2)}(\mathbf{r},\mathbf{r}')\rangle_\rho-\left(\frac{3\Gamma}{2\kappa^2}+\frac{\kappa\Gamma}{2}\right). \tag{A13}$$

For isotropic and homogeneous system,

$$\langle\delta^{(2)}(\mathbf{r},\mathbf{r}')\rangle_\rho=\rho_i^2g_\rho(|\mathbf{r}-\mathbf{r}'|),\qquad=\rho_i^2[h_\rho(|\mathbf{r}-\mathbf{r}'|)+1], \tag{A14}$$

where g_ρ and h_ρ are the radial pair-distribution and pair-correlation functions associated to the given phase space

density ρ, respectively. Consequently, the excess internal energy per particle due to interaction is simply given by

$$\left\langle \frac{\beta \mathcal{H}_Y}{N} \right\rangle_\rho = \frac{\rho_i}{2} \int d^3\mathbf{r} \beta v_Y(|\mathbf{r}|) h_\rho(|\mathbf{r}|) - \frac{\kappa\Gamma}{2}. \quad \text{(A15)}$$

Note that we would have obtained the same Eq. (A15) averaging Eq. (A7) and using the one-particle density $\delta^{(1)}(\mathbf{r})$, with $\langle \delta^{(1)}(\mathbf{r}) \rangle_\rho = \rho_i$ for isotropic and homogeneous system [15]. In the right-hand side of Eq. (A15), the first term is the expected quadrature formula and the second term is a correction coming from the zero of energy. h_ρ appears instead of g_ρ due to background. Equation (12) results combining Eqs. (A6) and (A15).

Now, let us calculate excess internal energy $u_Y^{(ex)} = \beta \mathcal{U}_Y^{(ex)}/N$, excess pressure $p_Y^{(ex)} = \beta \mathcal{P}_Y/\rho_i - 1$, and excess entropy $s_Y^{(ex)} = \mathcal{S}_Y^{(ex)}/(Nk_B)$ from Eq. (12). By definition,

$$\mathcal{P}_Y = -\left.\frac{\partial \mathcal{F}_Y}{\partial \Omega}\right|_T,$$

$$\mathcal{S}_Y = -\left.\frac{\partial \mathcal{F}_Y}{\partial T}\right|_\Omega,$$

$$\mathcal{U}_Y = \mathcal{F}_Y - \left.\frac{\partial \mathcal{F}_Y}{\partial T}\right|_\Omega = \left.\frac{\partial(\beta \mathcal{F}_Y)}{\partial \beta}\right|_\Omega \quad \text{(A16)}$$

at fixed particle number N. We know that $\mathcal{F}_Y$ can always be divided into an ideal part $\mathcal{F}^0$ and an excess part $\mathcal{F}_Y^{(ex)}$, i.e.,

$$\mathcal{F}_Y = \mathcal{F}^0 + \mathcal{F}_Y^{(ex)}. \quad \text{(A17)}$$

The expression of $\mathcal{F}^0$ is given in Eq. (A3). We have the same additive splitting for entropy, internal energy, and pressure, i.e.,

$$\mathcal{P}_Y = \mathcal{P}^0 + \mathcal{P}_Y^{(ex)},$$

$$\mathcal{S}_Y = \mathcal{S}^0 + \mathcal{S}_Y^{(ex)},$$

$$\mathcal{U}_Y = \mathcal{U}^0 + \mathcal{U}_Y^{(ex)}. \quad \text{(A18)}$$

Since our system of interest is in thermodynamic equilibrium at fixed particle number N, we can employ inverse temperature β and particle number ρ_i as state variables instead of temperature T and volume Ω. The chain rules for partial differentiation are thus simply given by

$$\Omega \left.\frac{\partial}{\partial \Omega}\right|_T = -\rho_i \left.\frac{\partial}{\partial \rho_i}\right|_\beta,$$

$$T \left.\frac{\partial}{\partial T}\right|_\Omega = -\beta \left.\frac{\partial}{\partial \beta}\right|_{\rho_i}. \quad \text{(A19)}$$

This choice is consistent with the thermodynamic limit implicitly assumed in the end (i.e., $N \to \infty$, $\Omega \to \infty$, $N/\Omega = \rho_i$) and is well adapted to the calculation of reduced thermodynamic functions. As an illustration, let us find the expression of the ideal reduced free energy $f^0 = \beta \mathcal{F}^0/N$, internal energy $u^0 = \beta \mathcal{U}^0/N$, entropy $s^0 = \mathcal{S}^0/(Nk_B)$, and pressure $p^0 = \beta \mathcal{P}^0/\rho_i$. From Eq. (A3), we easily have

$$f^0 = \ln(\rho_i) + \frac{3}{2}\ln(\beta) + \frac{3}{2}\ln\left(\frac{2\pi\hbar^2}{m}\right) - 1, \quad \text{(A20)}$$

and thus

$$\rho_i \left.\frac{\partial f^0}{\partial \rho_i}\right|_\beta = 1,$$

$$\beta \left.\frac{\partial f^0}{\partial \beta}\right|_{\rho_i} = \frac{3}{2}. \quad \text{(A21)}$$

Then, making $\mathcal{F}_Y^{(ex)} = 0$ in Eq. (A16) and using Eqs. (A19), (A20), and (A21), we get

$$\mathcal{P}^0 = \frac{\rho_i}{\beta} \rho_i \left.\frac{\partial f^0}{\partial \rho_i}\right|_\beta,$$

$$\mathcal{S}^0 = Nk_B \left(\beta \left.\frac{\partial f^0}{\partial \beta}\right|_{\rho_i} - f^0 \right),$$

$$\mathcal{U}^0 = \frac{N}{\beta} \beta \left.\frac{\partial f^0}{\partial \beta}\right|_{\rho_i}, \quad \text{(A22)}$$

or

$$p^0 = 1,$$

$$u^0 = \frac{3}{2},$$

$$s^0 = (u^0 - f^0). \quad \text{(A23)}$$

One can check that Eq. (A4) is recovered. Finally, $u_Y^{(ex)}$, $p_Y^{(ex)}$, and $s_Y^{(ex)}$ are simply obtained by keeping the term $\mathcal{F}_Y^{(ex)}$ in Eq. (A16) and following the same procedure. We get

$$\mathcal{P}_Y = \frac{\rho_i}{\beta} \rho_i \left.\frac{\partial (f^0 + f_Y^{(ex)})}{\partial \rho_i}\right|_\beta,$$

$$\mathcal{S}_Y = Nk_B \left[\beta \left.\frac{\partial (f^0 + f_Y^{(ex)})}{\partial \beta}\right|_{\rho_i} - (f^0 + f_Y^{(ex)}) \right],$$

$$\mathcal{U}_Y = \frac{N}{\beta} \beta \left.\frac{\partial (f^0 + f_Y^{(ex)})}{\partial \beta}\right|_{\rho_i}, \quad \text{(A24)}$$

or

$$p_Y^{(ex)} = \rho_i \left.\frac{\partial f_Y^{(ex)}}{\partial \rho_i}\right|_\beta,$$

$$u_Y^{(ex)} = \beta \left. \frac{\partial f_Y^{(ex)}}{\partial \beta} \right|_{\rho_i},$$

$$s_Y^{(ex)} = u_Y^{(ex)} - f_Y^{(ex)}. \tag{A25}$$

Of course, the left-hand side of Eq. (12) is unknown, but the GBI allows us to minimize the right-hand side of Eq. (12), i.e.,

$$\Delta f_\rho^{(ex)} \equiv f_\rho^{(ex)} - u_\rho^{(ex)} + \frac{\rho_i}{2} \int d^3\mathbf{r} \beta v_Y(|\mathbf{r}|) h_\rho(|\mathbf{r}|) - \frac{\kappa\Gamma}{2}, \tag{A26}$$

with respect to the given set of parameters $\{\alpha_n\}$ characterizing the reference system (Γ_{OCP} for OCP and η for HS). The minimum value of $\Delta f_\rho^{(ex)}$,

$$\Delta f_\rho^{(ex),0} \equiv \Delta f_\rho^{(ex)}|_{\{\alpha_n^0\}}, \tag{A27}$$

where the optimum parameters $\{\alpha_n^0\}$ satisfy the equations

$$\frac{\partial [\Delta f_\rho^{(ex)}]}{\partial \alpha_n} (\{\alpha_n^0\}) = 0, \tag{A28}$$

serves as an approximation of $f_Y^{(ex)}$. But it can be used to estimate various thermodynamic quantities, such as $u_Y^{(ex)}$, $p_Y^{(ex)}$, and $s_Y^{(ex)}$:

$$p_Y^{(ex)} \approx \rho_i \left. \frac{\partial \Delta f_\rho^{(ex),0}}{\partial \rho_i} \right|_\beta,$$

$$u_Y^{(ex)} \approx \beta \left. \frac{\partial \Delta f_\rho^{(ex),0}}{\partial \beta} \right|_{\rho_i},$$

$$s_Y^{(ex)} \approx u_Y^{(ex)} - \Delta f_\rho^{(ex),0}. \tag{A29}$$

Now, for the Yukawa system, the whole variables of interest depend on $\{\Gamma, \kappa\}$. It is thus convenient to express all lengths in unit of the Wigner-Seitz radius a_{WS} to have dimensionless quantities. Equations (A26) and (A29) read

$$\Delta f_\rho^{(ex)} = f_\rho^{(ex)} - u_\rho^{(ex)} + \frac{3}{2} \int_0^\infty dr r^2 u_Y(r) h_\rho(r) - \frac{\kappa\Gamma}{2}, \tag{A30}$$

and

$$p_Y^{(ex)} \approx \frac{\Gamma}{3} \left. \frac{\partial \Delta f_\rho^{(ex),0}}{\partial \Gamma} \right|_\kappa + \rho_i \left. \frac{\partial \kappa}{\partial \rho_i} \right|_\beta \left. \frac{\partial \Delta f_\rho^{(ex),0}}{\partial \kappa} \right|_\Gamma,$$

$$u_Y^{(ex)} \approx \Gamma \left. \frac{\partial \Delta f_\rho^{(ex),0}}{\partial \Gamma} \right|_\kappa + \beta \left. \frac{\partial \kappa}{\partial \beta} \right|_{\rho_i} \left. \frac{\partial \Delta f_\rho^{(ex),0}}{\partial \kappa} \right|_\Gamma,$$

$$s_Y^{(ex)} \approx u_Y^{(ex)} - \Delta f_\rho^{(ex),0}, \tag{A31}$$

using

$$\rho_i \left. \frac{\partial \Gamma}{\partial \rho_i} \right|_\beta = \frac{\Gamma}{3},$$

$$\beta \left. \frac{\partial \Gamma}{\partial \beta} \right|_{\rho_i} = \Gamma, \tag{A32}$$

and the most general case, in which κ depends both on ρ_i and β. When calculating $p_Y^{(ex)}$ and $u_Y^{(ex)}$ from Eq. (A31), only explicit differentiation with respect to Γ and κ are kept due to the GBI variational principle. One simply finds

$$p_Y^{(ex)} \approx -\frac{1}{2} \int_0^\infty dr r^2 h_\rho(r) \left(-1 + 3\rho_i \left. \frac{\partial \kappa}{\partial \rho_i} \right|_\beta r \right) u_Y(r) - \frac{\Gamma}{2} \left(\frac{\kappa}{3} + \rho_i \left. \frac{\partial \kappa}{\partial \rho_i} \right|_\beta \right),$$

$$u_Y^{(ex)} \approx \frac{3}{2} \int_0^\infty dr r^2 h_\rho(r) \left(1 - \beta \left. \frac{\partial \kappa}{\partial \beta} \right|_{\rho_i} r \right) u_Y(r) - \frac{\Gamma}{2} \left(\kappa + \beta \left. \frac{\partial \kappa}{\partial \beta} \right|_{\rho_i} \right). \tag{A33}$$

In our case, the Yukawa system is supposed to be given and no assumptions are done concerning the physical processes that create the screening. The inverse screening length is constant; this means that

$$\rho_i \left. \frac{\partial \kappa}{\partial \rho_i} \right|_\beta = -\frac{\kappa}{3},$$

$$\beta \left. \frac{\partial \kappa}{\partial \beta} \right|_{\rho_i} = 0. \tag{A34}$$

One thus recovers the standard formulas [15] to calculate excess pressure and excess internal energy, with the additional term due to the zero of energy:

$$p_Y^{(ex)} \approx -\frac{\rho_i}{6} \int d^3\mathbf{r} h_\rho(r) r \beta v_Y'(r),$$

$$u_Y^{(ex)} \approx \frac{\rho_i}{2} \int d^3\mathbf{r} h_\rho(r) \beta v_Y(r) - \frac{\Gamma\kappa}{2}. \tag{A35}$$

The radial pair-correlation function is calculated with the optimum set of parameters $\{\alpha_n^0\}$. It is by now clear that we cannot use the excess pressure and the excess internal energy of the reference system. The situation is more complicated in the general case when $\kappa = \kappa(\rho_i, \beta)$. As for entropy, the situation is very simple and opposite to what just encountered, because $s_Y^{(ex)}$ may be approximated by the entropy of the reference system $f_\rho^{(ex),0} - u_\rho^{(ex),0}$.

TABLE VI. Compressibility factor z as a function of the HS packing fraction η proposed by Carnahan and Starling [16] (CS) and by Erpenbeck and Wood [53] (EW). V-PY and C-PY are the virial and the compressibility expressions issuing from the Percus-Yevick approximation [15].

Model	V-PY	C-PY	CS	EW
$z(\eta)$	$\frac{1+2\eta+3\eta^2}{(1-\eta)^2}$	$\frac{1+\eta+\eta^2}{(1-\eta)^3}$	$\frac{1+\eta+\eta^2-\eta^3}{(1-\eta)^3}$	$1+\eta\frac{4+0.890851\eta+0.8924486\eta^2+0.3430298\eta^3}{1-2.277287\eta+1.3262418\eta^2}$

APPENDIX B: GBI EQUATIONS USING HS REFERENCE SYSTEM FOR YUKAWA SYSTEM

In this appendix, we derive practical formulas to minimize the right-hand side of Eq. (12) with respect to η at fixed $\{\Gamma,\kappa\}$. This is equivalent of finding the minimum of function $\eta\rightarrow\Delta\mathcal{F}^{GBI}_{\Gamma,\kappa}(\eta)$ defined in Eq. (14) at fixed $\{\Gamma,\kappa\}$. The approximations concern the two basic points of the theory, namely, the equation of state and the radial distribution function. In short, we extend the standard formulas originally proposed for the one-component Coulomb system to the one-component Yukawa system.

A large number of theoretical and phenomenological equations have been proposed for the HS equation of state (see for instance Ref. [53]). For simplicity, we have considered the well-known formula found by Carnahan and Starling [16] and the expression proposed more recently by Erpenbeck and Wood [53]. Both are simple and match nearly exactly the computer-generated equation of state. Moreover, an empirical formula for expressing the bridge function in terms of interparticle separation and density has been presented that is fully consistent with the best computer-simulation thermodynamics and structural data for HS in the fluid region at the time [54], i.e., the expression of Erpenbeck and Wood [53]. We give in Table VI the various relations for the HS equations of state, i.e., the ratio of the pressure to the ideal gas pressure P/P_0 (or compressibility factor z) as a function of the HS packing fraction η.

The HS radial distribution function taken in the Percus-Yevick (PY) approximation is known to suffer from two major defects [15]. On one hand, the value at contact is too small. On the other hand, the later oscillations have the wrong phase and are too weakly damped. Verlet and Weiss [17] and then, Henderson and Grundke [18], proposed to correct those defects. Both approaches are the same in their spirit. The main assumption consist is writting the radial distribution function $g_{HS}(r)$ as follows:

$$g_{HS}(r)=\begin{cases}0 & \text{if } r<\sigma_0\\ g_0(r/\sigma_0,\eta_0)+\dfrac{C_1}{(r/\sigma)}\exp[-C_2(r/\sigma-1)]\cos[-C_2(r/\sigma-1)] & \text{otherwise,}\end{cases} \tag{B1}$$

where $g_0(r/\sigma_0,\eta_0)$ is the PY expression for the radial distribution function [55,56]. σ_0 and η_0 are the corresponding HS diameter and packing fraction, respectively ($\eta_0=\pi\rho_i\sigma_0^3/6$); η_0 is related to η by the empirical formula [17,18]

$$\eta_0=\eta-\frac{\eta^2}{16}. \tag{B2}$$

The parameters C_1 and C_2 are chosen so that the equations of state calculated from either the pressure equation,

$$z(\eta)\equiv 1+f(\eta)=1+4\eta g_{HS}(\sigma), \tag{B3}$$

or the compressibility equation,

$$\frac{\partial[\eta z(\eta)]}{\partial\eta}=\frac{1}{1+\rho_i\int_0^\infty dr\,4\pi r^2[g_{HS}(r)-1]}, \tag{B4}$$

are equal to the equation of state given by the function $f(\eta)$. The integral in Eq. (B4) can be done analytically using [57]

$$\int_0^\infty dx x^2[g_0(x,\eta_0)-1]=\frac{(\eta_0-4)(\eta_0^2+2)}{24(1+2\eta_0)^2} \tag{B5}$$

to yield

$$\frac{1}{z(\eta)+\eta\dfrac{\partial z(\eta)}{\partial\eta}}=\frac{(1-\eta_0)^4}{(1+2\eta_0)^2}+12\eta\frac{C_1}{C_2}-24\eta_0\int_1^{(\eta/\eta_0)^{1/3}}dx x^2 g_0(x,\eta_0). \tag{B6}$$

Equation (B3) determines the parameter C_1,

$$C_1=\frac{f(\eta)}{4\eta}-g_0[(\eta/\eta_0)^{1/3},\eta_0], \tag{B7}$$

whereas the parameter C_2 is fixed by Eq. (B6).

Algebraic calculations are easier if we use (i) the Laplace transform of $x[g_0(x,\eta_0)-1]$ [55,56]

$$\int_0^\infty dx x e^{-\alpha x}[g_0(x,\eta_0)-1]=G(\alpha,\eta_0)-\alpha^{-2}\equiv\mathcal{G}(\alpha,\eta_0), \tag{B8}$$

where

$$G(x,\eta_0)=\frac{xe^{-x}H(x,\eta_0)}{12\eta[e^{-x}H(x,\eta_0)+I(x,\eta_0)]}, \tag{B9}$$

with

$$H(x,\eta_0)=12\eta_0[x(1+\eta_0/2)+2\eta_0+1],$$

$$I(x,\eta_0)=(1-\eta_0)^2x^3+6\eta_0(1-\eta_0)x^2+18\eta_0^2x-12\eta_0(1+2\eta_0), \tag{B10}$$

and (ii) the Wertheim analytical expression for $g_0(x,\eta_0)$ [55]. For our purpose, since $0<\eta_0<1$ for $0<\eta<1$, it is sufficient to know this expression for $0<x<1$ only:

$$xg_0(x,\eta_0)=(1-\eta_0)^{-2}\sum_{l=0}^{2}A_l e^{t_l(x-1)}, \tag{B11}$$

where

$$A_l=\frac{1}{3}\sum_{m=0}^{2}H_m j^{ml}, \tag{B12}$$

and

$$H_0=1+\frac{\eta}{2},$$

$$H_1=-(4\eta)^{-1}\left(f^2+\frac{1}{8}\right)^{-1/2}\left[x_-^2(1-3\eta-4\eta^2)+x_+\times\left(1-\frac{5}{2}\eta^2\right)\right],$$

$$H_2=(4\eta)^{-1}\left(f^2+\frac{1}{8}\right)^{-1/2}\left[x_+^2(1-3\eta-4\eta^2)+x_-\times\left(1-\frac{5}{2}\eta^2\right)\right]. \tag{B13}$$

Here $j=e^{2\pi i/3}$, $f=(3+3\eta-\eta^2)/(4\eta^2)$, $x_\pm=\pm|f\pm(f^2+1/8)^{1/2}|^{1/3}$, and $t_l=2\eta(-1+x_+j^l+x_-j^{-l})/(1-\eta)$. Note that the result concerning $x_\pm$ is misprint in the original [55], as in other references [57–59], if not simply absent; it is correctly given in this paper. The VW solution differs from the HG approach by making good but irrelevant approximations. The parameters C_1 and C_2 are simple functions of η_0

$$C_1=\frac{3}{4}\frac{\eta_0^2(1-0.7117\eta_0-0.114\eta_0^2)}{(1-\eta_0)^4},$$

$$C_2=\frac{24C_1(1-\eta_0)^2}{\eta_0(1+\eta_0/2)}, \tag{B14}$$

but the formulas are restricted to the CS equation of state. In summary, when an accurate equation of state is used, the resulting radial distribution function obtained from those developments fits the "exact" computer-generated (Monte Carlo or molecular dynamics) functions to within one percent for all η [15].

Using Eqs. (B1), (B6), and (B7), it is thus a simple task to calculate $\eta\to\Delta f_{\Gamma,\kappa}^{GBI}(\eta)$ defined in Eq. (14). Since $f_{HS}^{(ex)}=\int_0^\eta dx f(x)/x$ and $\mathcal{U}_{HS}^{(ex)}=0$,

$$\Delta f_{\Gamma,\kappa}^{GBI}(\eta)=\int_0^\eta dx\frac{f(x)}{x}+6\Gamma\left[\eta_0^{2/3}\mathcal{G}(\alpha_0,\eta_0)+\eta^{2/3}\frac{C_1e^{-\alpha}(\alpha+C_2)}{(\alpha+C_2)^2+C_2^2}-\eta_0^{2/3}\int_1^{(\eta/\eta_0)^{1/3}}dx x e^{-\alpha_0 x}g_0(x,\eta_0)\right]-\frac{\Gamma\kappa}{2}, \tag{B15}$$

where $\alpha_0=2\eta_0^{1/3}\kappa$ and $\alpha=2\eta^{1/3}\kappa$. Note that this expression is badly formatted for numerical purpose at small κ. One should rather use a Taylor expansion with respect to α and α_0 in this situation and make sure that the one-component Coulomb system case is recovered when the CS equation of state and the PY radial distribution function are used [36].

Expressions of excess entropy $s_Y^{(ex)}$, excess internal energy $u_Y^{(ex)}$, and excess pressure $p_Y^{(ex)}$ are easily derived from Eq. (B15) using Appendix A,

$$s_Y^{(ex)}=-\int_0^\eta dx f(x)/x,$$

$$u_Y^{(ex)}=6\Gamma\left[\eta_0^{2/3}\mathcal{G}(\alpha_0,\eta_0)+\eta^{2/3}\frac{C_1e^{-\alpha}(\alpha+C_2)}{(\alpha+C_2)^2+C_2^2}-\eta_0^{2/3}\int_1^{(\eta/\eta_0)^{1/3}}dx x e^{-\alpha_0 x}g_0(x,\eta_0)\right]-\frac{\Gamma\kappa}{2},$$

$$p_Y^{(ex)}=\frac{1}{3}\left(u_Y^{(ex)}-\kappa\frac{\partial u_Y^{(ex)}}{\partial\kappa}\right). \tag{B16}$$

Here, we only have to consider explicit differentiation with respect to κ due to the variational character of the equations.

[1] N.W. Ashcroft and D. Stroud, Solid State Phys. **33**, 1 (1978).
[2] S. Galam and J.-P. Hansen, Phys. Rev. A **14**, 816 (1976).
[3] H. Iyetomi, K. Utsumi, and S. Ichimaru, J. Phys. Soc. Jpn. **50**, 3769 (1981).
[4] S. Tanaka and S. Ichimaru, Phys. Rev. A **35**, 4743 (1987).
[5] M.S. Murillo, Phys. Rev. E **62**, 4115 (2000).
[6] J. Clérouin and J.-F. Dufrêche, Phys. Rev. E **64**, 66 406 (2001).
[7] U. Konopka, G.E. Morfill, and L. Ratke, Phys. Rev. Lett. **84**, 891 (2000).
[8] J.C. Crocker and D.G. Grier, Phys. Rev. Lett. **73**, 352 (1994).
[9] S. Hamaguchi, R.T. Farouki, and D.H.E. Dubin, J. Chem. Phys. **105**, 7641 (1996); S. Hamaguchi, R.T. Farouki, and D.H.E. Dubin, Phys. Rev. E **56**, 4671 (1997).
[10] J.M. Caillol and D. Gilles, J. Stat. Phys. **100**, 905,933 (2000).
[11] H. Ohta and S. Hamaguchi, Phys. Plasmas **7**, 4506 (2000).
[12] T. Saigo and S. Hamaguchi, Phys. Plasmas **9**, 1210 (2002).
[13] G. Salin and J.M. Caillol, Phys. Rev. Lett. **88**, 065002 (2002).
[14] R.P. Feynman, *Statistical Mechanics* (Addison-Wesley, New York, 1992).
[15] J.-P. Hansen and I.R. McDonald, *Theory of Simple Liquids*, 2nd ed. (Academic Press, London, 1986).
[16] N.F. Carnahan and K.E. Starling, J. Chem. Phys. **53**, 600 (1970).
[17] L. Verlet and J.J. Weiss, Phys. Rev. A **5**, 939 (1972).
[18] D. Henderson and E.W. Grundke, J. Chem. Phys. **63**, 601 (1975).
[19] W.L. Slattery, G.D. Doolen, and H.E. DeWitt, Phys. Rev. A **21**, 2087 (1980); W.L. Slattery, G.D. Doolen, and H.E. DeWitt, *ibid.* **26**, 2255 (1982); G.S. Stringfellow, H.E. DeWitt, and W.L. Slattery, *ibid.* **41**, 1105 (1990).
[20] D.A. Young, E.M. Corey, and H.E. DeWitt, Phys. Rev. A **44**, 6508 (1991).
[21] H.E. DeWitt and W.L. Slattery, Contrib. Plasma Phys. **39**, 97 (1999).
[22] B. Held and P. Pignolet, J. Phys. (France) **47**, 437 (1986).
[23] J.-L. Bretonnet and A. Derouiche, Phys. Rev. B **38**, 9255 (1988).
[24] F.J. Rogers, D.A. Young, H.E. DeWitt, and M. Ross, Phys. Rev. A **28**, 2990 (1983).
[25] K.-C. Ng, J. Chem. Phys. **61**, 2680 (1974).
[26] Y. Rosenfeld and N.W. Ashcroft, Phys. Rev. A **20**, 1208 (1979).
[27] F.J. Rogers and D.A. Young, Phys. Rev. A **30**, 999 (1984).
[28] G. Zérah and J.-P. Hansen, J. Chem. Phys. **84**, 2336 (1986).
[29] Y. Rosenfeld, J. Stat. Phys. **42**, 437 (1986).
[30] H. Iyetomi, S. Ogata, and S. Ichimaru, Phys. Rev. A **46**, 1051 (1992).
[31] Y. Rosenfeld, J. Stat. Phys. **94**, 929 (1998).
[32] W.H. Press, S.A. Teukolski, W.T. Vetterling, and B.P. Flannery, *Numerical Recipes in Fortran: The Art of Scientific Computing*, 2nd ed. (Cambridge University Press, New York, 1992).
[33] S. Bonazzola, E. Gourgoulhon, and J.-A. Marck, J. Comput. Appl. Math. **109**, 433 (1999).
[34] Y. Rosenfeld, Phys. Rev. A **46**, 1059 (1992).
[35] Y. Rosenfeld, Phys. Rev. E **53**, 2000 (1996).
[36] D. Stroud and N.W. Ashcroft, Phys. Rev. A **13**, 1660 (1976).
[37] W.G. Hoover and F.H. Ree, J. Chem. Phys. **49**, 3609 (1968).
[38] F. Perrot and G. Chabrier, Phys. Rev. A **43**, 2879 (1991).
[39] J.-P. Hansen, I.R. McDonald, and E.L. Pollock, Phys. Rev. A **11**, 1025 (1975).
[40] Y. Rosenfeld, Phys. Rev. A **15**, 2545 (1977).
[41] Y. Rosenfeld, J. Phys.: Condens. Matter **11**, 5415 (1999).
[42] Y. Rosenfeld, Phys. Rev. E **62**, 7524 (2000).
[43] Y. Rosenfeld, J. Phys.: Condens. Matter **13**, L39 (2001).
[44] J.J. Erpenbeck and W.W. Wood, Phys. Rev. A **43**, 4254 (1991).
[45] J. Wallenborn and M. Baus, Phys. Rev. A **18**, 1737 (1978).
[46] Z. Donko and B. Nyiri, Phys. Plasmas **7**, 45 (2000).
[47] B.J. Alder, D.M. Gass, and T.M. Wainwright, J. Chem. Phys. **53**, 3813 (1970).
[48] I.M. de Schepper, A.F.E.M. Haffmans, and H. van Beijeren, Phys. Rev. Lett. **57**, 1715 (1986).
[49] B. Bernu and P. Vieillefosse, Phys. Rev. A **18**, 2345 (1978).
[50] R. Grover, W.G. Hoover, and B. Moran, J. Chem. Phys. **83**, 1255 (1985).
[51] S. Chapman and T.G. Cowling, *The Mathematical Theory of Non-Uniform Gases* (Cambridge University Press, New York, 1952).
[52] R. Cauble and D.B. Boercker, Phys. Rev. A **28**, 944 (1983).
[53] J.J. Erpenbeck and W.W. Wood, J. Stat. Phys. **35**, 321 (1984).
[54] A. Malijevský and S. Labík, Mol. Phys. **60**, 663 (1987).
[55] M.S. Wertheim, Phys. Rev. Lett. **10**, 321 (1963); M.S. Wertheim, J. Math. Phys. **5**, 643 (1964).
[56] E. Thiele, J. Chem. Phys. **39**, 474 (1963).
[57] W.R. Smith and D. Henderson, Mol. Phys. **19**, 411 (1970).
[58] G.A. Mansoori, J.A. Provine, and F.B. Canfield, J. Chem. Phys. **51**, 5295 (1969).
[59] G.J. Throop and R.J. Bearman, J. Chem. Phys. **42**, 2408 (1964).